Cell Reports

Article

Sex-biased islet β cell dysfunction is caused by the MODY MAFA S64F variant by inducing premature aging and senescence in males

Graphical abstract

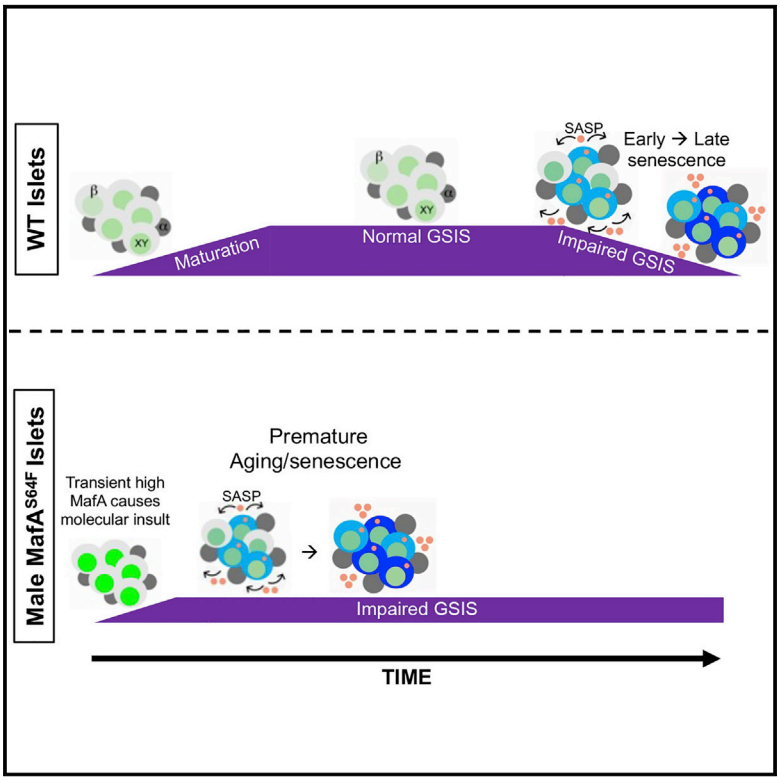

Highlights

- *MafA*$^{S64F/+}$ mice show sex-dependent β cell dysfunction (diabetes or hypoglycemia)
- *MafA*$^{S64F/+}$ male and female mice show aberrant islet Ca^{2+} signaling
- Only *MafA*$^{S64F/+}$ males show markers of islet aging and senescence
- MAFA^{S64F} expression in male human EndoC-βH2 cells accelerates cellular senescence

Authors

Emily M. Walker, Jeeyeon Cha, Xin Tong, ..., John Stafford, David A. Jacobson, Roland Stein

Correspondence

roland.stein@vanderbilt.edu

In brief

Walker et al. show that mice harboring the missense mutation of the pancreatic islet-enriched transcription factor MAFA (S64F MAFA) demonstrate sex-dependent β cell dysfunction, similar to findings in human carriers. Only male S64F MAFA β cells show accelerated senescence and β cell dysfunction toward hyperglycemia.

Walker et al., 2021, Cell Reports *37*, 109813
October 12, 2021
https://doi.org/10.1016/j.celrep.2021.109813

CellPress

Cell Reports

CellPress
OPEN ACCESS

Article

Sex-biased islet β cell dysfunction is caused by the MODY MAFA S64F variant by inducing premature aging and senescence in males

Emily M. Walker,[1,9] Jeeyeon Cha,[2] Xin Tong,[1] Min Guo,[1] Jin-Hua Liu,[1] Sophia Yu,[2] Donato Iacovazzo,[3] Franck Mauvais-Jarvis,[4,5,8] Sarah E. Flanagan,[6] Márta Korbonits,[3] John Stafford,[1,2,7] David A. Jacobson,[1] and Roland Stein[1,10,*]

[1]Department of Molecular Physiology and Biophysics, Vanderbilt University, Nashville, TN, USA
[2]Division of Diabetes, Endocrinology, and Metabolism, Department of Medicine, Vanderbilt University Medical Center, Nashville, TN, USA
[3]Centre for Endocrinology, Barts and The London School of Medicine, Queen Mary University of London, London EC1M 6BQ, UK
[4]Section of Endocrinology and Metabolism, Department of Medicine, Tulane University Health Sciences Center, New Orleans, LA, USA
[5]Southeast Louisiana Veterans Healthcare System, New Orleans, LA, USA
[6]Institute of Biomedical and Clinical Science, University of Exeter Medical School, Exeter EX2 5DW, UK
[7]Tennessee Valley Healthcare System, Veterans Affairs, Nashville, TN, USA
[8]Tulane Center of Excellence in Sex-Based Biology & Medicine, Tulane University Health Sciences Center, New Orleans, LA, USA
[9]Present address: Division of Metabolism, Endocrinology, and Diabetes, Department of Internal Medicine, University of Michigan Medical School, Ann Arbor, MI, USA
[10]Lead contact
*Correspondence: roland.stein@vanderbilt.edu
https://doi.org/10.1016/j.celrep.2021.109813

SUMMARY

A heterozygous missense mutation of the islet β cell-enriched MAFA transcription factor (p.Ser64Phe [S64F]) is found in patients with adult-onset β cell dysfunction (diabetes or insulinomatosis), with men more prone to diabetes than women. This mutation engenders increased stability to the unstable MAFA protein. Here, we develop a S64F MafA mouse model to determine how β cell function is affected and find sex-dependent phenotypes. Heterozygous mutant males (*MafA*$^{S64F/+}$) display impaired glucose tolerance, while females are slightly hypoglycemic with improved blood glucose clearance. Only *MafA*$^{S64F/+}$ males show transiently higher MafA protein levels preceding glucose intolerance and sex-dependent changes to genes involved in Ca^{2+} signaling, DNA damage, aging, and senescence. MAFA^{S64F} production in male human β cells also accelerate cellular senescence and increase senescence-associated secretory proteins compared to cells expressing MAFA^{WT}. These results implicate a conserved mechanism of accelerated islet aging and senescence in promoting diabetes in MAFA^{S64F} carriers in a sex-biased manner.

INTRODUCTION

The large V-Maf avian musculoaponeurotic fibrosarcoma transcription factor MafA is a pancreatic β cell-enriched protein that is essential for activating rodent transcriptional programs to promote β cell maturation and function, as can be measured by glucose-stimulated insulin secretion (GSIS) (Artner et al., 2008, 2010; Hang and Stein, 2011; Hang et al., 2014; Zhang et al., 2005). The presence of MafA in only insulin$^+$ β cells during islet cell development and postnatally distinguishes it from other important islet cell-enriched regulators (Golson and Kaestner, 2017; Hang and Stein, 2011; Pan and Wright, 2011; Shih et al., 2013). For example, transcription factors such as Pdx1 and Nkx6.1, which are expressed earlier and more broadly, also have a profound impact on pancreas organogenesis, islet β cell function, and whole-body glucose homeostasis in mice (Madsen et al., 1997; Pan and Wright, 2011). Pdx1 is present in both the exocrine and endocrine pancreas during development and then principally in islet β cells postnatally (Pan and Wright, 2011), while Nkx6.1 is found in endocrine progenitors and is later restricted to β cells (Golson and Kaestner, 2017; Hang and Stein, 2011; Pan and Wright, 2011; Shih et al., 2013).

In contrast, mice lacking MafA (i.e., *MafA*$^{-/-}$ (Zhang et al., 2005), *MafA*$^{\Delta panc}$ (Artner et al., 2010; Hang et al., 2014), and *MafA*$^{\Delta\beta}$ (Cyphert et al., 2019; Luan et al., 2019) have normal pancreas formation and a relatively subtle influence on postnatal physiology, primarily compromising GSIS in a sex-independent manner. However, MafA has been proposed to play a distinct late role in postnatal islet β cell maturation, in part supported by observations demonstrating that inducing MafA expression levels in normally non-glucose-responsive and MafA^{Low} neonatal rat islets increases GSIS (Aguayo-Mazzucato et al., 2011), while compromising levels reduce mouse (Artner et al., 2010; Cyphert et al., 2019; Hang et al., 2014; Luan et al., 2019; Zhang et al., 2005) and human (Guo et al., 2013) β cell activity. A key regulatory role is also implied by the ability of many islet-enriched transcription factors to coordinately

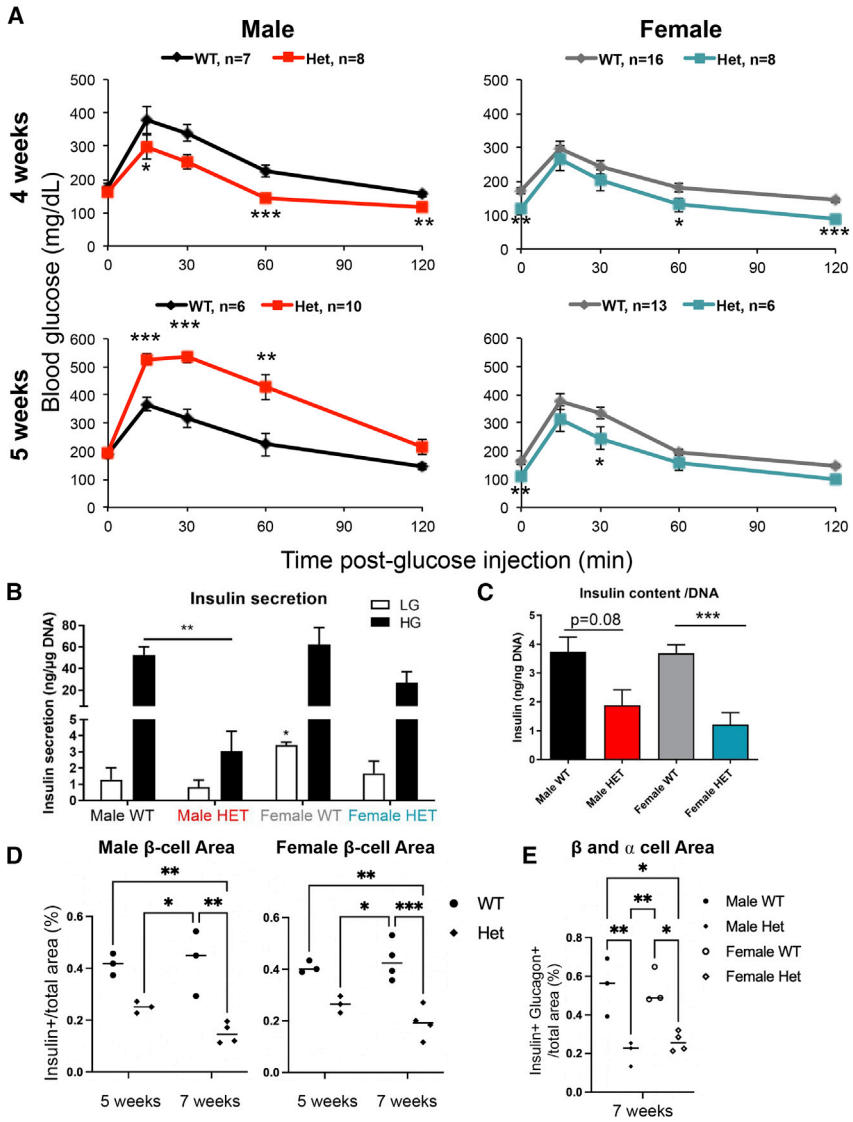

Figure 1. Male but not female *MafA*$^{S64F/+}$ mice become glucose intolerant between 4 and 5 weeks of age

(A) Fasted male and female animals underwent intraperitoneal glucose tolerance tests at 4 and 5 weeks of age. Male heterozygous (termed Het) *MafA*$^{S64F/+}$ mice (red line) had improved glucose clearance at 4 weeks but become glucose intolerant by 5 weeks. Female *MafA*$^{S64F/+}$ mice (teal line) had significantly lower fasting blood glucose levels and improved glucose clearance at both time points.

(B) High glucose-stimulated insulin secretion in isolated islets was impaired in male *MafA*$^{S64F/+}$ samples at 5 weeks. Islets were incubated with 4.6 mM (low, LG) or 16.8 mM (high, HG) glucose for 1 h. Secreted insulin was normalized to DNA content.

(C) Islet insulin content trended lower in *MafA*$^{S64F/+}$ males and was significantly decreased in females. Levels were normalized to DNA content.

(D) Male (left panel) and female (right panel) islet β cell area was reduced at 7 weeks in *MafA*$^{S64F/+}$ mice. The area was calculated by dividing the total insulin^{+} area by the total pancreatic area (eosin staining) in pancreas sections obtained every 50 μm multiplied by 100 to obtain percentage (%).

(E) Indicative of reduced islet area, the combined islet β and α cell area was significantly reduced in male and female *MafA*$^{S64F/+}$ mice at 7 weeks.

(A–C) Two-tailed Student t test; *p < 0.05; **p < 0.01; ***p < 0.001.

(D and E) Two-way ANOVA; *p < 0.05; **p < 0.01; ***p < 0.005.

stimulate *MafA* gene transcription, including Pdx1 and Nkx6.1 (Raum et al., 2006, 2010).

Expression of MafB, the other large Maf family member produced in the islet, differs from MafA in being produced in both murine α and β cells developmentally (Cyphert et al., 2019; Hang and Stein, 2011), then postnatally only in α cells and a subpopulation of maternal β cells during pregnancy (Banerjee et al., 2016; Cyphert et al., 2019). Moreover, genetic studies have demonstrated that MafB is dispensable in regulating adult murine islet β cell function, except during pregnancy (Banerjee et al., 2016; Cyphert et al., 2019). MafA expression during mouse β cell development compensates for the absence of MafB, although glucagon secretion from islet α cells is compromised (Conrad et al., 2016). In addition, misexpressing MafB in *MafA*$^{\Delta panc}$ β cells cannot rescue MafA function (Cyphert et al., 2019). These results illustrate similarities and differences between MafA and MafB in expression and function in rodent islet cells.

While most islet-enriched transcription factors are produced in an analogous fashion in rodents and humans, there are unique differences in the temporal and islet cell type-specific expression pattern of the human MAFA and MAFB proteins. In humans, MAFA protein is not detected in the β cell until ~10 years of age, while MAFB is present throughout the lifespan of human insulin^{+} β cells (Cyphert et al., 2019; Dai et al., 2012). These observations imply that humans have at least two postnatal β cell populations (in terms of MAFA) capable of maintaining euglycemia, represented by the juvenile (i.e., <10 years old and MAFA^{Low}:MAFB^{+}) and post-juvenile (≥10 years old and MAFA^{High}:MAFB^{+}) periods. In fact, independent studies have established distinct molecular and functional properties of these temporally produced human cell populations (Arda et al., 2016; Arrojo E Drigo et al., 2019; Camunas-Soler et al., 2020) and an association between MAFA levels and adult islet β cell functional heterogeneity (Chen et al., 2019). MAFA and MAFB levels are reduced in type 2 diabetic (T2D) islets (Guo et al., 2013), and (at least) MAFA is particularly sensitive to oxidative stress and glucotoxic conditions (Harmon et al., 2005). While the role of MAFA or MAFB has not been analyzed directly in intact human islets, both are required for GSIS in the human EndoC-βH1 β cell line (Scharfmann et al., 2014; Scoville et al., 2015). Moreover, we

have recently shown that MAFB is essential to insulin production in human embryonic stem cell-derived β cells (Russell et al., 2020), which is in stark contrast to its dispensable role in rodents (Banerjee et al., 2016; Cyphert et al., 2019). These findings highlight species-specific differences in MAFA and MAFB production and islet cell distribution, likely implying that the homodimeric MAFB activator and the MAFA:MAFB heterodimeric activator provide unique functional characteristics to human islet β cells.

Individuals carrying a heterozygous mutation in the MAFA transactivation domain producing a substitution of the conserved serine at position 64 with a phenylalanine (p.Ser64Phe [S64F]) develop either diabetes mellitus or insulinomatosis, a non-syndromic condition of hyperinsulinemic hypoglycemia caused by multiple insulin-secreting neuroendocrine tumors. The mean age at diagnosis for both conditions is 38 years (Iacovazzo et al., 2018). These results demonstrate that MAFA is a causative gene for maturity-onset diabetes of the young (MODY), a collection of monogenic diseases predominantly driven by mutations in essential islet-enriched transcription factors (Barbetti and D'Annunzio, 2018). Interestingly, diabetes is prevalent in male MAFA^{S64F} carriers (i.e., 3:1), while insulinomatosis is more common in female carriers (4:1) (Iacovazzo et al., 2018). *In vitro* analysis demonstrated that the S64F substitution prevents a key priming phosphorylation event at position S65 in MAFA, which profoundly increases the stability of the normally unstable MAFA protein by affecting processes necessary for ubiquitin-mediated degradation (Iacovazzo et al., 2018).

Due to the rare detection of MAFA^{S64F}-mediated diseases and difficulty of performing mechanistic studies in a human context, we used CRISPR-Cas9-based mutagenesis to establish a mouse model (termed *MafA*$^{S64F/+}$) harboring the same pathogenic single base pair substitution (C>T) as human carriers. Diabetes-related phenotypes were specifically associated with male *MafA*$^{S64F/+}$ heterozygous mice by 5 weeks of age, which manifested glucose intolerance due in part to a reduced glucose-stimulated β cell Ca^{2+} response. These changes were preceded by an overt but transient increase in MafA protein levels in islet β cells at 4 weeks. In addition, the functional deficiencies in male *MafA*$^{S64F/+}$ islet β cells accompanied the induction of markers of DNA damage, cell-cycle exit, senescence, and the senescence-associated secretory phenotype (SASP) at 5 weeks, consistent with accelerated cellular aging and senescence. In contrast, heterozygous mutant female mice not only had lower fasting blood glucose levels and improved glucose clearance but also did not display any of the overt aging and senescence signatures of littermate, heterozygous males. Expression of MAFA^{S64F} in the male human β cell line, EndoC-βH2, showed increased senescent gene markers and secretion of human-specific SASP factors capable of inducing senescence in a cell non-autonomous manner. These results indicate that diabetes in human male *MAFA*^{S64F} carriers is caused by the premature senescence and aging of islet β cells.

RESULTS

Male *MafA*$^{S64F/+}$ mice are glucose intolerant due to impaired insulin secretion

Since MafA is a primary regulator of glucose clearance and insulin secretion in islet β cells (Hang and Stein, 2011), *MafA*$^{S64F/+}$ and wild-type (WT) littermates were subjected to glucose tolerance testing (GTT) and fasting blood glucose measurements at various postnatal time points. While both male and female *MafA*$^{S64F/+}$ animals had improved glucose clearance at 4 weeks, females also had modest fasting hypoglycemia (Figure 1A). Strikingly, male *MafA*$^{S64F/+}$ animals developed persistent glucose intolerance beginning at 5 weeks of age, while females continued to have improved glucose tolerance and lower fasting blood glucose levels (Figure 1A). GTT results were stably maintained in male and female *MafA*$^{S64F/+}$ mice (Figure S1). The sex-dependent male phenotype was even more penetrant in homozygous *MafA*$^{S64F/S64F}$ mutants, as males displayed overt diabetes with elevated fasting glucose levels that progressively worsened (Figures S2A and S2B). In contrast, the phenotype of homozygous females was much more variable and largely comparable to WT littermates (Figure S2C). Because of the generally poor survival of homozygous mutants postnatally (Figure S2D), possibly resulting from severe neurodevelopmental defects due to *MafA*$^{S64F/S64F}$ expression and its altered activity in the central nervous system (Lecoin et al., 2010; Niceta et al., 2015), all of the remaining experimentation was performed with male and female heterozygous *MafA*$^{S64F/+}$ mice.

Insulin secretion by *ex vivo* GSIS was impaired in 5-week-old male *MafA*$^{S64F/+}$ islets (Figure 1B), although insulin content trended lower in male *MafA*$^{S64F/+}$ islets and was significantly reduced in female islets (Figure 1C). *MafA*$^{S64F/+}$ female mice appear to have lower fasting blood glucose levels (Figure 1A) due to increased insulin secretion in both low (5.6) and high (16.7) glucose conditions as determined by dynamic perifusion assays (Figure S3A) and increased fasting serum insulin levels (Figure S3B). Thus, 8- to 10-week old female *MafA*$^{S64F/+}$ islets had markedly improved 1st and 2nd phase GSIS properties compared to controls in the perifusion assays, while males *MafA*$^{S64F/+}$ islets showed a mild improvement in this *ex vivo* system, but not nearly to the levels found in females (Figure S3C). Because of the counterregulatory effects of insulin on glucagon hormone secretion (Franklin et al., 2005), we considered that glucose-regulated glucagon levels may be altered in *MafA*$^{S64F/+}$ mice. However, there was neither an obvious sex-dependent impact on glucose-stimulated glucagon secretion nor a change in glucagon content (Figures S3D and S3E). The islet α cell area was also unchanged in both male and female *MafA*$^{S64F/+}$ islets, although this was variable among animals (Figure S3F).

The insulin^{+} β cell area was reduced in male and female *MafA*$^{S64F/+}$ mice (Figure 1D), as were their combined β and α cell areas and β cell number per islet section (Figures 1E and S3H). The decrease in β cell area may be due to lower islet cell proliferation rates in *MafA*$^{S64F/+}$ mice relative to WT littermates (Figure S3G). In addition, the changes in blood glucose levels were not attributable to differences in peripheral tissue insulin sensitivity or glucose uptake as insulin tolerance tests and glycogen storage were both unchanged (Figures S4A and S4B). Animal body weight was also not appreciably altered in *MafA*$^{S64F/+}$ mice, except for a small decrease in female *MafA*$^{S64F/+}$ mice at 5 weeks of age that disappeared by 6 weeks (Figure S4C). These combined results suggested a fundamental difference(s) in *MafA*$^{S64F/+}$ β cell activity between the sexes, resulting in their distinguishing ability to control glucose homeostasis.

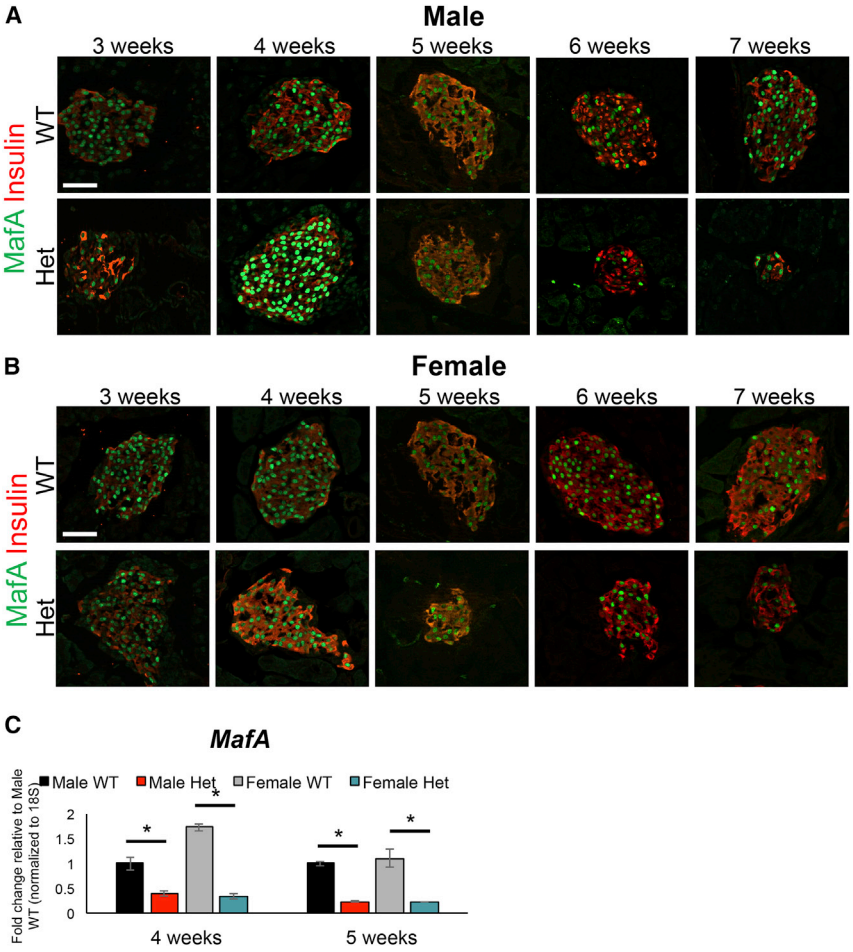

Figure 2. MAFA protein levels were transiently upregulated at 4 weeks in male *MafA*$^{S64F/+}$ islets

(A) Immunostaining over the course of 3, 4, 5, 6, and 7 weeks revealed that MAFA protein staining intensity only increased at 4 weeks of age in male *MafA*$^{S64F/+}$ (Het) islets.

(B) In contrast, MAFA staining intensity was unchanged between female *MafA*$^{S64F/+}$ and WT islets.

(C) *MafA* mRNA levels were significantly reduced at 4 and 5 weeks in both male and female *MafA*$^{S64F/+}$ islet samples. Fold change shown relative to male WT islets. Two-tailed Student t test; *p < 0.05; scale bars, 50 μm.

MafA protein levels are transiently and profoundly upregulated before the changes in glucose clearance in male *MafA*$^{S64F/+}$ islet β cells

The MAFA^{S64F} variant impairs a key, priming phosphorylation event at position S65, which blocks subsequent glycogen synthase kinase 3 (GSK3)-mediated phosphorylation at positions S61, T51, T57, and S49 in the transactivation domain. These changes impede ubiquitin-mediated protein degradation of MAFA^{S64F}, and its stability is dramatically increased when expressed in the human EndoC-βH1 β cell line (Han et al., 2007; Iacovazzo et al., 2018; Rocques et al., 2007). Consequently, we predicted that this mutation in the highly conserved region of the protein (Han et al., 2007; Iacovazzo et al., 2018; Rocques et al., 2007) would also increase MafA levels in *MafA*$^{S64F/+}$ β cells. Surprisingly, we only found elevated MafA protein immunostaining intensity in male *MafA*$^{S64F/+}$ islets at 4 weeks of age (Figure 2A), 1 week before the onset of glucose intolerance (Figure 1A). In contrast, MafA protein levels were not increased in female *MafA*$^{S64F/+}$ β cells at 4 weeks or any other analyzed time point (Figure 2B). However, there was a roughly 3- to 5-fold decrease in *MafA* transcript levels at 4 and 5 weeks of age in both male and female *MafA*$^{S64F/+}$ islets compared to WT littermates (Figure 2C). The reduction in *MafA* gene expression indicates that the more stable MafA^{S64F} protein is acting in an autoregulatory manner, likely by binding at the conserved MafA binding site within the 5′-flanking sequences of the Region 3 transcription control domain (Raum et al., 2010).

Because the sex hormones estradiol and testosterone affect islet cell function (Gannon et al., 2018), we questioned whether these hormones influenced the sex-biased phenotypes in *MafA*$^{S64F/+}$ mice. Both sexes achieved puberty appropriately with fertility comparable to WT littermates (data not shown). Female *MafA*$^{S64F/+}$ mice were ovariectomized to investigate whether estrogen was regulating mutant sex-biased activity. As expected, ovariectomy at 3 weeks of age produced glucose intolerance in WT female mice by 4 weeks of age (Figure S5A). In contrast, glucose tolerance was unaffected by ovariectomy in age-matched female *MafA*$^{S64F/+}$ mice (data not shown; Figure S5A). These results indicate that the effects of the MafA^{S64F} variant is dominant over the effects of estrogen deficiency on glucose intolerance. Furthermore, testosterone levels were not altered markedly in *MafA*$^{S64F/+}$ males at both 4 and 5 weeks of age and were similar to age-matched females in these pre- and peripubertal mice (Figure S5B). The low circulating levels of testosterone produced during this phenotypic window lowers the likelihood of this hormone influencing MafA^{S64F} actions.

Collectively, these results strongly suggest that MafA^{S64F} regulates male and female islet β cells through common and distinct mechanisms; however, these processes are not principally influenced by the primary sex hormones.

Glucose- and potassium chloride (KCl)-stimulated calcium handling were altered in both male and female *MafA*$^{S64F/+}$ islets

To provide an unbiased and comprehensive perspective over how MafA^{S64F} influences islet β cell gene expression, bulk RNA sequencing (RNA-seq) was performed on isolated islets from 5-week-old WT and *MafA*$^{S64F/+}$ male and female mice when a clear delineation of phenotypes was observed. Female heterozygous islets had 736 differentially expressed genes (DEGs) (337 up

and 399 down) compared to female WT islets, while males had 2,410 DEGs (2,031 up and 379 down) (Figure 3A). There were also 391 DEGs that were similarly regulated between the sexes, which were revealed by Gene Ontology analysis as having $p < 0.05$ and included factors associated with Ca^{2+} and K^+ channels important in controlling β cell function (Figures 3B and 3C). In addition, other voltage-dependent Ca^{2+} channel genes as well as genes important to ion influx were also specifically upregulated in male *MafA*$^{S64F/+}$ islets (Figure 3D), suggesting both sex-dependent and sex-independent changes in ion flux in *MafA*$^{S64F/+}$ islets.

Since glucose-induced elevations of cytoplasmic Ca^{2+} mediate insulin release (Bergsten et al., 1994), WT and *MafA*$^{S64F/+}$ islet Ca^{2+} handling was monitored in response to glucose stimulation and KCl-induced depolarization. As expected from the GSIS response of male *MafA*$^{S64F/+}$ islets (Figures 1B and S3C), their Ca^{2+} entry was significantly blunted relative to the WT islets in response to 11 mM glucose stimulation (Figure 4A; represented by red trace in left panel and called a "non-responder"). The glucose-stimulated Ca^{2+} oscillatory pattern that is responsible for pulsatile insulin secretion was also significantly diminished in these *MafA*$^{S64F/+}$ islets (Figure 4A). In contrast, there appeared to be two distinct Ca^{2+} responsive islet populations in female *MafA*$^{S64F/+}$ animals. One was similar to male *MafA*$^{S64F/+}$ islets in having a very limited initial glucose response and minimal oscillatory behavior (i.e., Figure 4A, dark green representative trace in right panel and labeled a non-responder). However, the remaining islets had more subtle decreases in their initial response to 11 mM glucose, and subsequently oscillate with higher frequency but equivalent amplitude to WT islets (Figure 4A, "responders," teal representative trace in right panel). The average peak amplitude of the initial glucose-induced Ca^{2+} response was reduced in all male and female *MafA*$^{S64F/+}$ islets (Figure 4B). This suggests that the *MafA*$^{S64F/+}$ female islet responders population is able to compensate for the non-responders and maintain glucose tolerance in *MafA*$^{S64F/+}$ female mice, which would be predicted because only a fraction (roughly 20%) of the β cell mass is thought to be required to maintain glucose tolerance (Gale, 2002).

Male and female *MafA*$^{S64F/+}$ islets also had disparate Ca^{2+} responses to KCl-mediated depolarization. The KCl-induced Ca^{2+} influx (ΔCa^{2+} after KCl application divided by baseline Ca^{2+}) was significantly reduced in male *MafA*$^{S64F/+}$ islets when compared to WT male islets (Figures 4C and S5C). Interestingly, however, the female *MafA*$^{S64F/+}$ islets showed greater KCl-induced Ca^{2+} influx when compared to WT female islets, which was observed for both glucose-stimulated Ca^{2+} responders and non-responders (Figures 4C, S3A, and S5C). Importantly, female *MafA*$^{S64F/+}$ islets also showed greater baseline (5 mM glucose) Ca^{2+} levels than WT female islets (Figure S5D), which is consistent with the fasting hypoglycemia and increased fasting insulin levels observed in female *MafA*$^{S64F/+}$ mice (Figures 1A and S3B).

Only male *MafA*$^{S64F/+}$ islets express markers of accelerated cellular senescence and aging

Because 5-week-old male *MafA*$^{S64F/+}$ islet β cells were not only defined by a predominant, Ca^{2+} non-responsive population (Figures 4A and 4B) but also by glucose intolerance (Figure 1A), we focused our attention on identifying molecular determinants to their poor function. In addition to the previously illustrated gene expression alterations involved in Ca^{2+} signaling (index ranking 6, Figure 5A), 5-week-old male *MafA*$^{S64F/+}$ RNA-seq data revealed the upregulation of many metabolic pathway genes implicated in cellular aging (e.g., index ranking pathways 4, 6, and 8) and senescence (e.g., index ranking pathways 1, 2, 3, 5, 6, 7, and 8 in Figure 5A) (Basisty et al., 2018; Campisi and d'Adda di Fagagna, 2007; Coppé et al., 2010; Franceschi et al., 2018; Greenhill, 2019; Kabir et al., 2016; Mancini et al., 2012; Martin and Bernard, 2018). Furthermore, the preponderance of upregulated genes detected by RNA-seq implied that MafA^{S64F} is acting as a dominant activator in (at least) male *MafA*$^{S64F/+}$ islets (Figure 3A).

Cellular senescence is a durable, cell-cycle arrest response that regulates cell fate specification, tissue patterning, and function during development, cell maturation, and organismal aging (Campisi, 2014; Gorgoulis et al., 2019; Helman et al., 2016; Herranz and Gil, 2018). It is also induced in a variety of disease states and primarily serves as a stress response to many internal and external insults (Gorgoulis et al., 2019; Herranz and Gil, 2018). The importance of premature aging and senescence in driving male *MafA*$^{S64F/+}$ β cell dysfunction was supported by the many genes associated with these responses, including those controlling Ca^{2+} signaling (Figure 3D), aging (Figure 5B), the DNA damage response (DDR; Figure 5C), SASP (Figure 5D), and cytokine-cytokine receptor interactions (Figure 5E). As expected, the expression of candidate genes linked to aging and senescence were increased in 5-week-old male *MafA*$^{S64F/+}$ islets (Figure 5F), although not before manifesting glucose intolerance in 4-week-old males (Figures 1A and 5F). Importantly, these genes were largely unaltered in *MafA*$^{S64F/+}$ female islets (Figure S6A), although many other female candidate DEGs were validated by qPCR (Figures 3D, 5B–5F, S6B, and S6C).

Senescent cells undergo a progression of changes after an initial insult: early initiation of cellular arrest by activation of cell-cycle inhibitors (e.g., p53, p21, and/or p16) and DDR responses in an attempt to regain homeostasis (Gorgoulis et al., 2019; Herranz and Gil, 2018). DDR can be characterized by markers such as phosphorylated histone H2AX (gH2AX) and 53BP1 recruitment to chromatin. We identified increased immunostaining for the gH2AX marker for DNA double-strand breaks, the P53 binding protein-1 (53BP1) DNA damage marker (Schultz et al., 2000), and the p21 cell-cycle arrest and senescence marker (Fang et al., 1999) in 5-week-old *MafA*$^{S64F/+}$ male, but not female islets (Figures 6A–6C and S7A–S7C). While only 3% of the male WT islets showed >10% p21$^+$ β cells, this proportion increased to 37% (including 15% with >20% p21$^+$ β cells) in male *MafA*$^{S64F/+}$ islets (Figure 6C, right panel).

Apoptosis was not induced in response to DNA damage in either male or female *MafA*$^{S64F/+}$ islets, as determined by the inability to detect islet TUNEL$^+$ cells between 4 and 7 weeks of age (data not shown; Figure S7F). Induction of anti-apoptosis genes (e.g., the BCL2 family members; Figure 5F) and resistance to apoptosis are consistent with the senescence phenotype (Herranz and Gil, 2018; Thompson et al., 2019). In fact, key markers of senescence, such as decreases in LaminB1 mRNA and protein (Figure 6D) (Freund et al., 2012) and increased endogenous senescence-associated β-galactosidase (SA-β-gal) staining was detected in male *MafA*$^{S64F/+}$ islets at levels

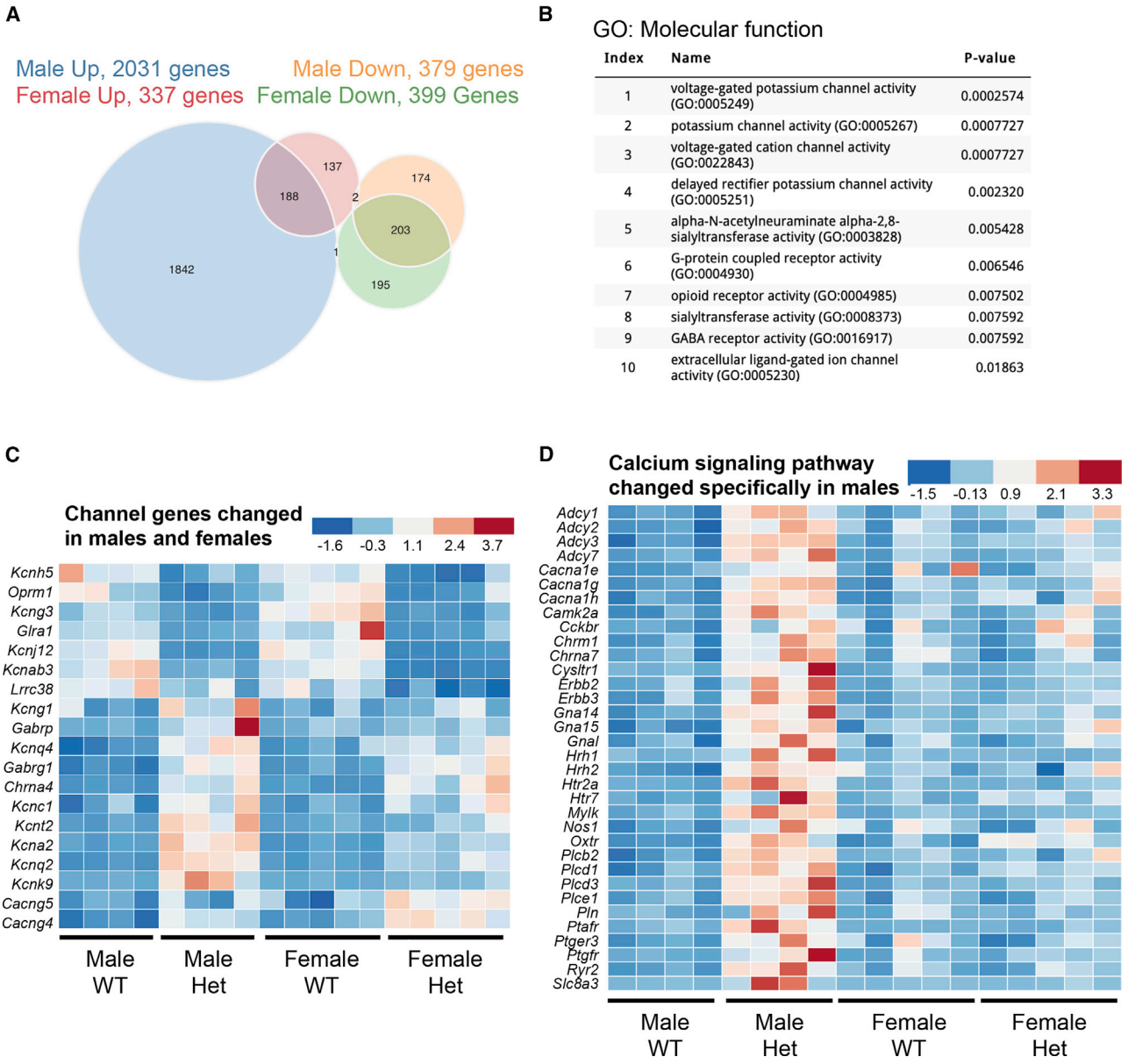

Figure 3. Male and female *MafA*$^{S64F/+}$ islet cells regulate a common and distinct set of genes associated with Ca^{2+} and K^+ channel activity

(A) The Venn diagram illustrates the total number of RNA-seq-identified genes differentially up- or down-regulated between 5-week-old WT and *MafA*$^{S64F/+}$ islets.

(B) Gene Ontology (GO): molecular function analysis ($p < 0.05$) of the 391 genes commonly up- or down-regulated in *MafA*$^{S64F/+}$ (Het) islets revealed alterations in multiple ion channel activity pathways.

(C) Heatmaps showing channel gene expression changes common between male and female *MafA*$^{S64F/+}$ islets.

(D) Heatmap of Ca^{2+} signaling pathway genes uniquely increased in male *MafA*$^{S64F/+}$ islets identified by Kyoto Encyclopedia of Genes and Genomes (KEGG) analysis (also see Figure 5A). False discovery rate (FDR) < 0.05.

comparable to mice aged 10–12 months (Figures 6E and 6F). Notably, SA-β-gal was undetectable at 4 weeks in male *MafA*$^{S64F/+}$ islets, a time point before β cell dysfunction or ever in female *MafA*$^{S64F/+}$ islets, nor was LaminB1 expression decreased in female *MafA*$^{S64F/+}$ islets (Figures 6D–6F, and S7D and S7E). These results illustrate a novel sex-dependent pathophysiology of accelerated β cell aging and senescence that contributes to glucose intolerance in *MafA*$^{S64F/+}$ males.

Human EndoC-βH2 β cells expressing MAFA^{S64F} show increased markers of cellular senescence and a functional senescence-associated secretory phenotype

Human EndoC-βH2 cells were transduced with human MAFA^{WT} or MAFA^{S64F} expression constructs using lentivirus to investigate whether cellular senescence could be prematurely induced in human β cells. Immunoblot analysis of protein extracts from these EndoC-βH2 cells confirmed the

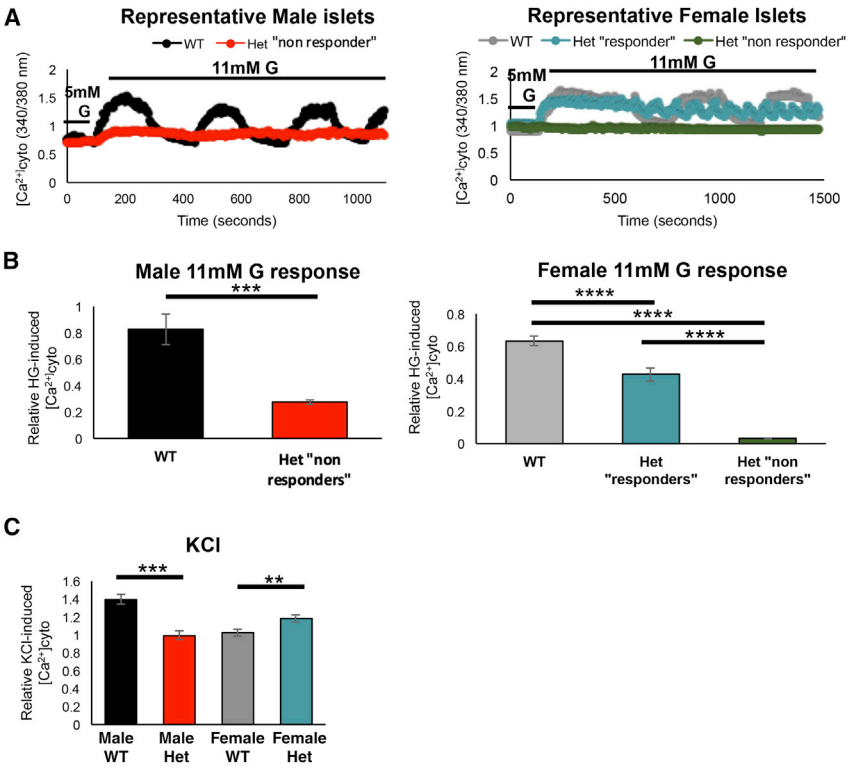

Figure 4. Glucose-induced Ca^{2+} oscillations and KCl-induced Ca^{2+} responses are altered in *MafA*$^{S64F/+}$ islets

(A) Representative Fura2 traces show loss of the β cell glucose-induced Ca^{2+} oscillations (11 mM glucose [G]) in 5-week-old male *MafA*$^{S64F/+}$ (Het) islets (red line, "non-responders"). Female *MafA*$^{S64F/+}$ islets had 2 different functionally responsive islet populations ("responders," teal line; non-responders, green line).

(B) Quantitation of male (left; 2-tailed Student t test; ***$p < 0.001$) and female (right; 1-way ANOVA; ****$p < 0.0001$) islets showed reduced cytoplasmic Ca^{2+} following stimulation with 11 mM glucose. The average peak amplitude was quantitated by dividing the first peak ΔCa^{2+} after 11 mM glucose application by the baseline response at 5 mM glucose.

(C) The Ca^{2+} response to 30 mM KCl is reduced in male *MafA*$^{S64F/+}$ islets but increased in female *MafA*$^{S64F/+}$ islets. Representative traces for this experiment are shown in Figure S8. Two-tailed Student t test; **$p < 0.01$; ***$p < 0.001$.

faster migrating properties of the phosphorylation-impaired MAFA^{S64F} (Figure S8A) (Iacovazzo et al., 2018). As in our *MafA*$^{S64F/+}$ mouse model, MAFA^{S64F}-producing cells had significantly increased SA-β-gal, p21, and 53BP1 expression and decreased LaminB1 expression compared to those expressing the human MAFA^{WT} protein (Figures 7A–7D and S8B). Gene expression analysis of MAFA^{S64F}-expressing β cells showed changes consistent with senescence markers identified in male *MafA*$^{S64F/+}$ mice (i.e., increased *p21*, increased *BCL2*, and decreased *LMNB1*) and decreased expression of *MAFB* (Figure 7C), a transcription factor not produced in rodent islet β cells postnatally (Conrad et al., 2016). As found in male *MafA*$^{S64F/+}$ mutant mouse islets, overexpressing MAFA^{S64F} in human EndoC-βH2 β cells caused misexpression of a number of critical calcium channel genes, including *CACNA1A*, *CACNA1C*, *CACNA1E*, and *CACNA1G* without altering insulin secretion machinery gene expression (Figure S8C).

Progression of senescence includes the development of SASP factors, which upon secretion induce senescence by reprogramming neighboring cells in a cell non-autonomous manner (Gorgoulis et al., 2019; Herranz and Gil, 2018). To determine whether SASP factors are released by human cells expressing MAFA^{S64F}, control medium or conditioned media (CM) collected from EndoC-βH2 cells expressing either MAFA^{WT} or MAFA^{S64F} was applied to untransduced EndoC-βH2 cells (Figure 7E). Notably, SASP genes identified in male *MafA*$^{S64F/+}$ mice were not increased in EndoC-βH2 cells in response to MAFA^{WT} or MAFA^{S64F} CM; however, human-specific SASP markers in gene families related to those identified in *MafA*$^{S64F/+}$ male mice were specifically increased by MAFA^{S64F} CM (Figure 7E). These results illustrate the ability of MAFA^{S64F} to promote cellular senescence in human β cells and to generate a functional, human β cell SASP via species-specific mediators.

DISCUSSION

Post-translational modifications of the islet-enriched MAFA protein are critical for regulating its activity, stability, and cellular localization for appropriate β cell function (Guo et al., 2009, 2010; Han et al., 2007; Iacovazzo et al., 2018; Rocques et al., 2007). Here, we have developed a mouse model of the human MAFA^{S64F} variant to understand mechanistically the sex-biased pathophysiological outcomes of MODY or insulinomatosis in affected heterozygous human carriers (Iacovazzo et al., 2018). Significantly, the physiological outcomes of *MafA*$^{S64F/+}$ mice appear to mimic the outcomes expected in human subjects, with glucose intolerance in males and improved glucose clearance and hypoglycemia in females.

This mutation blocks a key priming phosphorylation event at S65, which normally directs post-translational modifications affecting MAFA protein stability (Guo et al., 2009; Han et al., 2007; Rocques et al., 2007), transactivation (Han et al., 2007; Rocques et al., 2007), oncogenesis (Rocques et al., 2007), and DNA binding (Guo et al., 2010). These modifications are coupled to two antagonistic regulatory processes: increased transactivation activity and ubiquitin-mediated degradation (Rocques et al., 2007), illustrating that impeccable regulation of this protein is linked to islet β cell health. Earlier *in vitro* analysis demonstrated that the MAFA^{S64F} variant converted this normally unstable protein ($t_{1/2}$ ~30 min) to a very stable form ($t_{1/2} \geq 4$ h) (Iacovazzo et al., 2018). However, both male and female *MafA*$^{S64F/+}$ mice

A

KEGG analysis

Index	Name	P-value
1	Protein digestion and absorption_Homo sapiens_hsa04974	2.396e-9
2	ECM-receptor interaction_Homo sapiens_hsa04512	1.786e-7
3	Cytokine-cytokine receptor interaction_Homo sapiens_hsa04060	0.000003286
4	PI3K-Akt signaling pathway_Homo sapiens_hsa04151	0.00001506
5	Arachidonic acid metabolism_Homo sapiens_hsa00590	0.00001060
6	Calcium signaling pathway_Homo sapiens_hsa04020	0.00002454
7	Focal adhesion_Homo sapiens_hsa04510	0.00003833
8	AGE-RAGE signaling pathway in diabetic complications_Homo sapiens_hsa04933	0.00006126
9	Malaria_Homo sapiens_hsa05144	0.00005057
10	Amoebiasis_Homo sapiens_hsa05146	0.00005514

B

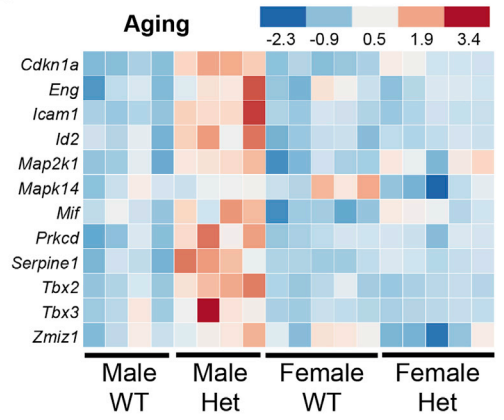

C

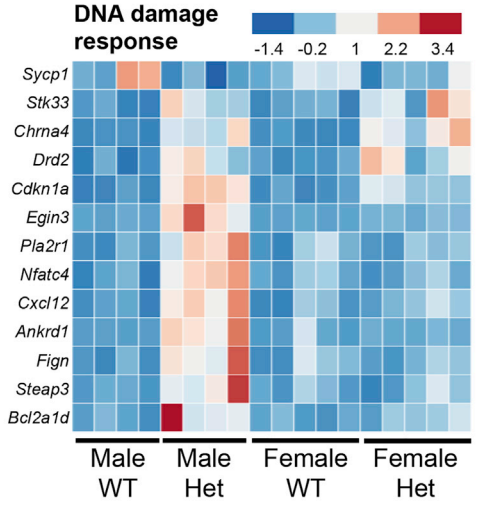

D

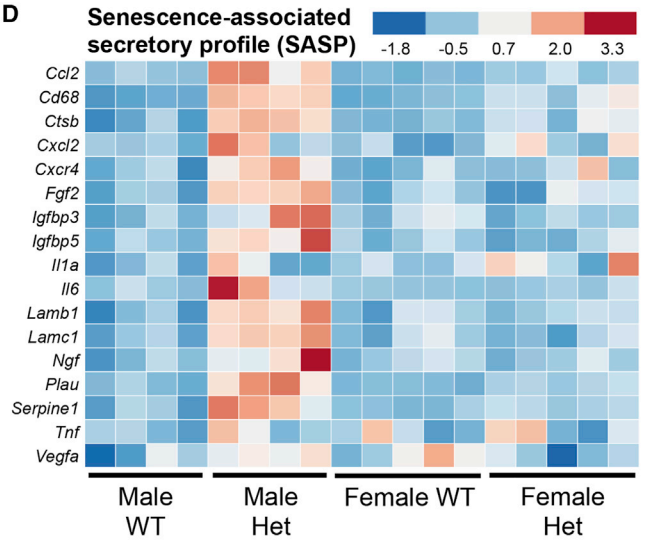

E

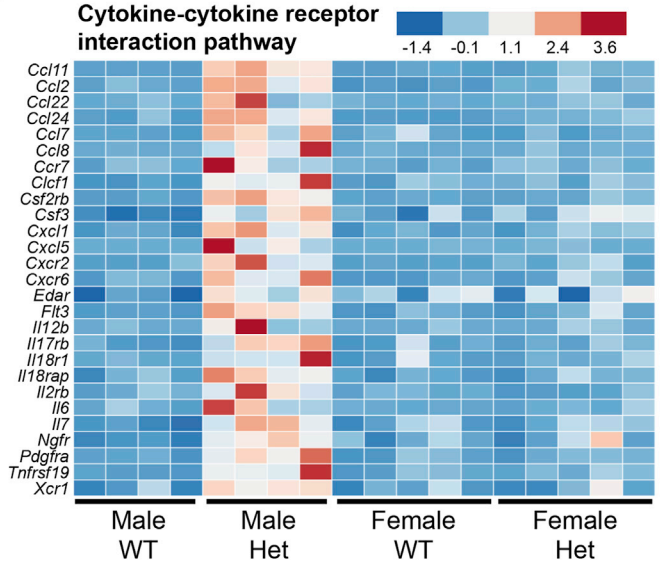

F

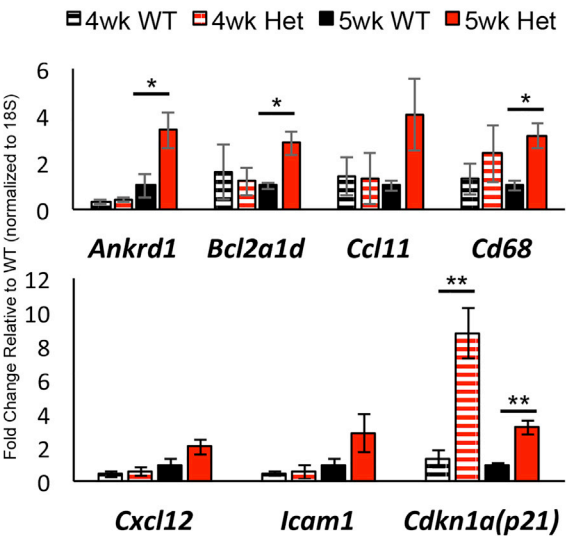

(legend on next page)

had similar improvements in glucose tolerance at 4 weeks, before overt and transient elevation in protein levels in only males (Figures 1 and 2). Notably, this increase in MafA^{S64F} protein levels preceded glucose intolerance seen by 5 weeks of age in males, while females continued to be modestly hypoglycemic, with improved glucose clearance. The changes in male and female *MafA*$^{S64F/+}$ β cell activity were maintained throughout the period of analysis despite the presence of WT-like protein levels after 5 weeks. However, we propose that MafA^{S64F} is more abundantly and persistently produced than MAFA^{WT} throughout the lifetime of the β cell despite similar protein levels because of 3- to 5-fold lower *MafA* mRNA levels in male and female *MafA*$^{S64F/+}$ islets in relation to the WT islets (Figure 2C). In line with this observation, human MAFA protein levels were largely unchanged by immunohistochemistry between the normal and insulinoma β cells of MAFA^{S64F} patients (Iacovazzo et al., 2018).

Our examination of ovariectomized female *MafA*$^{S64F/+}$ mice suggested that the estrogen sex hormone did not have a direct regulatory role, so it is presently unclear what factors are controlling the sexually dimorphic phenotypes of MafA^{S64F} mutant mice. Since MAFA^{S64F}-induced disease is not observed until ~38 years of age in both sexes without reports of affected pubertal development (Iacovazzo et al., 2018), we believe that neither estrogen nor testosterone have an impact on the divergent disease processes in humans. Instead, we propose that future efforts focus on determining whether sex chromosome-linked genes are influenced by MAFA^{S64F}, such as the X chromosome-linked candidate genes found differentially expressed in 5-week-old *MafA*$^{S64F/+}$ male islets (Figure S9A).

Bulk RNA-seq analysis of 5-week-old male and female *MafA*$^{S64F/+}$ mouse islets illustrated similar dysregulation of genes involved in β cell identity and ion channel function (Figures 3, S9B, and S9C). For example, the expression of several markers of β cell maturation were diminished in both *MafA*$^{S64F/+}$ male and female islets (Figures S9B and S9C), including the *Mnx1* (Pan et al., 2015) and *Pdx1* transcription factors as well as the *Ucn3* neuropeptide (van der Meulen et al., 2015). In addition, the expression of both sex-dependent and sex-independent genes involved in Ca^{2+} responses were identified (Figure 3). Accordingly, functional analyses after glucose stimulation revealed dysfunctional Ca^{2+} responses. While all male 5-week-old *MafA*$^{S64F/+}$ islets appear to have severely blunted glucose-induced Ca^{2+} responses (called non-responders in Figure 4), females contained both non-responder and unique responder islets with higher frequency oscillations in response to glucose. Presumably, responder islets mediate the high basal glucose-induced insulin secretion properties that are characteristic of female *MafA*$^{S64F/+}$ islets (Figures 4A and S3), while downstream effectors of Mnx1 and Pdx1 activation that are involved in cell signaling (e.g., *Gcgr*, *Glp1r*), secretion (*Syt2*, *Ucn3*, *Ins1*, *Ins2*), and ion channel activity contribute to β cell non-responder dysfunction (Blum et al., 2014; Gilbert and Blum, 2018; Jacobson and Shyng, 2020; Kalwat and Cobb, 2017).

Because of the heterogeneity of the Ca^{2+} signaling changes in female *MafA*$^{S64F/+}$ islets, we narrowed our focus to determine possible mechanisms contributing to the MafA^{S64F}-induced diabetic phenotype in males. Future single-cell sequencing efforts could reveal the factors regulating the interplay of distinct responder and non-responder islet β cell populations of *MafA*$^{S64F/+}$ females as well as their relative homogeneity in male non-responder islets. Importantly, our results clearly show that the many gene products associated with male *MafA*$^{S64F/+}$ β cell inactivity are not made in female heterozygotes (Figures 5 and S6). As divergent regulation of metabolism between the sexes in aging and disease is increasingly recognized (Sampathkumar et al., 2020), MAFA^{S64F} may provide a penetrant model to study sex-dependent effects on β cell health.

As expected, dynamic perifusion studies showed a marked reduction in baseline and stimulated insulin secretion in male compared to female *MafA*$^{S64F/+}$ islets (Figure S3). However, the mildly elevated insulin secretion levels of 10- to 12-week-old male *MafA*$^{S64F/+}$ islets appears at odds with the impairment in static insulin secretion at 5 weeks and temporally stable glucose intolerance levels (Figure 1). We propose that the age of the mutant mice may account for this discrepancy. Potentially, the older and more active male β cells "compensate" for the less active 5-week-old cells that were affected by the SASP factors secreted at the onset of glucose intolerance. Future studies will be focused on directly determining whether functionally and molecularly distinct β cell populations are progressively produced upon MAFA^{S64F} exposure.

Since Ca^{2+} release in *MafA*$^{S64F/+}$ male islets appeared to contribute to β cell inactivity, we focused on understanding how this process was affected in this context. Our results have demonstrated that MafA^{S64F} produces premature aging and senescence signatures in male murine β cells and human EndoC-βH2 cells (Figures 5, 6, and 7). In contrast, neither an aging nor senescence signature was observed in female murine β cells expressing MafA^{S64F} (Figures S6 and S7). Future studies will also investigate whether changes in Ca^{2+} handling occurs before or after *MafA*$^{S64F/+}$ male islets transition to a senescent phenotype as Ca^{2+} is also implicated in cellular senescence (Martin and Bernard, 2018).

Unlike the temporary cell-cycle arrest of quiescence, senescence is thought to be irreversible and refractory to mitogenic stimuli. Senescent cells undergo a progression of changes after early insult, including cell-cycle arrest by the activation of inhibitors (i.e., p53, p21, and/or p16, among others; Figures 5, 6, and 7) and DDR responses (Gorgoulis et al., 2019; Herranz and Gil, 2018). Progression to senescence involves chromatin remodeling to influence gene expression, metabolism, autophagy, and SASP, with the release of a heterogeneous mix of SASP effector

Figure 5. Male *MafA*$^{S64F/+}$ islets display increased expression of aging, DDR, SASP, and cytokine pathway gene signatures

(A) KEGG analysis of the 1,842 genes specifically upregulated in 5-week-old male *MafA*$^{S64F/+}$ (Het) islets.

(B–E) Heatmaps reveal male *MafA*$^{S64F/+}$ islets have increased expression of pathway genes associated with (B) aging, (C) DDR, (D) SASP, and (E) cytokine-cytokine receptor interactions. FDR < 0.05.

(F) qRT-PCR confirmation of pathway gene changes in 5-week-old male *MafA*$^{S64F/+}$ islets (solid bars). Gene expression was unchanged at 4-week-old male *MafA*$^{S64F/+}$ islets, with the exception of Cdkn1a (p21) upregulation (hash-marked bars). Two-tailed Student t test; *p < 0.05; **p < 0.01.

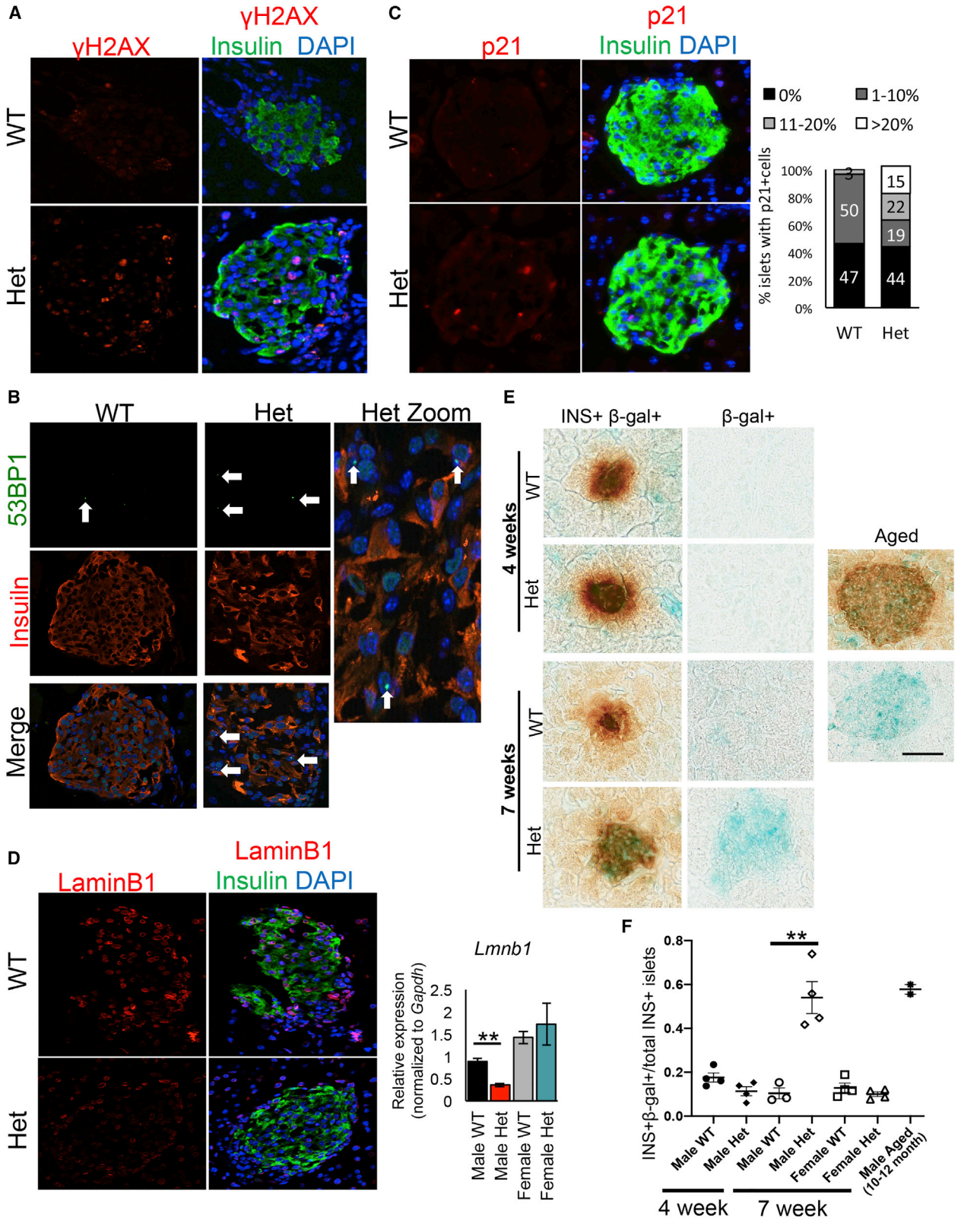

(legend on next page)

proteins influencing neighboring cells in a cell non-autonomous manner (Gorgoulis et al., 2019; Herranz and Gil, 2018). Terminal senescence from persistent damage involves autocrine and paracrine SASP amplification, loss of nuclear integrity, and diversification of the SASP phenotype (Gorgoulis et al., 2019). Notably, senescence-associated SA-β-gal staining was not induced in 4-week-old *MafA*$^{S64F/+}$ β cells, just 1 week before the detection of glucose intolerance (Figures 1 and 6).

Ultimately, senescent cells become resistant to apoptosis by the upregulation of anti-apoptotic proteins, such as those in the BCL2 family, and are often cleared by immune cells (Gorgoulis et al., 2019; Herranz and Gil, 2018). Interestingly, effective clearance of β cells is not apparent in *MafA*$^{S64F/+}$ male islets as we see accumulation of senescent cells, and there was no evidence of β cell death or immune cell infiltration (data not shown; Figures 6 and S7F). Senescent cells can play a causal role in aging-related pathology (van Deursen, 2014), and targeted removal of senescent cells can improve health span and reduce the incidence of aging-related diseases (Baker et al., 2011, 2016; Chang et al., 2016; Childs et al., 2016). Independent studies have shown that removal of the rare, senescent β cells in mouse models of T1D and T2D helps restore β cell function and glucose homeostasis *in vivo* (Aguayo-Mazzucato et al., 2019; Thompson et al., 2019). These senescent β cells showed distinct SASP signatures depending on modeling context (T1D versus T2D) (Aguayo-Mazzucato et al., 2019; Thompson et al., 2019), and these signatures were also species dependent such that only a subset of SASP mediators identified in respective mouse models were detected in human, diabetic islets (Aguayo-Mazzucato et al., 2019; Thompson et al., 2019).

Importantly, up to 50%–60% of human T2D β cells were shown to be senescent (Aguayo-Mazzucato et al., 2019), compared to their rare occurrence in previously described mouse models (Aguayo-Mazzucato et al., 2019; Thompson et al., 2019). This rate of β cell senescence is comparable to that found in *MafA*$^{S64F/+}$ male islets, suggesting that this variant models the widespread β cell senescence in human T2D (Figure 6). In fact, MAFA^{S64F} expression produced senescence in human EndoC-βH2 β cells with the development of a functional SASP. Treatment with CM from MAFA^{S64F}-expressing EndoC-βH2 cells induced β cell senescence and SASP factor expression differently from those identified in *MafA*$^{S64F/+}$ male mouse islets, albeit from similar molecular families. In summary, these studies implicate MAFA^{S64F}-induced senescence factors in causing β cell dysfunction and open doors to the identification of β cell senescence signatures across etiologies of diabetes (Figure 7F).

Human and rodent islets differ substantially in architecture, cell composition, proliferative capacity, islet amyloid formation, antioxidant enzyme levels, and, most significantly for the results described herein, MAFA and MAFB transcription factor expression (Bosco et al., 2010; Brissova et al., 2005; Butler et al., 2007; Cabrera et al., 2006; Dai et al., 2012; Fiaschi-Taesch et al., 2010; Henquin et al., 2006; Tyrberg et al., 2001). Because MafA is expressed at the onset of rodent β cell formation during embryogenesis, but not until 10 years of age in humans (Cyphert et al., 2019; Dai et al., 2012; Hang and Stein, 2011), we appreciate that some of the observations made in *MafA*$^{S64F/+}$ mice will not be directly relevant to the human disease. For example, since substantial β cell proliferation ceases in humans before MAFA expression (Cyphert et al., 2019; Dai et al., 2012; Hang and Stein, 2011), the decreased islet cell proliferation observed in male and female *MafA*$^{S64F/+}$ mice may not be directly relevant in humans. We also did not expect to find that *MafA*$^{S64F/+}$ male mice would manifest the overt fasting hyperglycemia seen in affected humans (Iacovazzo et al., 2018), since only 1 of the 7 human MODY transcription factors has a phenotype in heterozygous mice comparable to human carriers (i.e., Pdx1 (Ahlgren et al., 1998)). As found in other studies of MODY transcription factor function in mice, only the homozygous (male) *MafA*$^{S64F/S64F}$ mice manifested an explicit elevation in fasting blood glucose levels and glucose intolerance, which worsened with age (Figure S2). MafA^{S64F} presumably represents another example of how gene dosage of critical regulatory gene variants affects islet cell health in a species-specific manner.

It is also likely that the unique requirement of MAFB in human (but not rodent) β cells influences the effects of MAFA^{S64F} in human carriers. The human MAFA^{S64F}:MAFB heterodimeric activator could impart a unique influence on β cells compared to the mouse MafA^{S64F}:MafA homodimeric activator (Cyphert et al., 2019; Hang and Stein, 2011), which may explain why neuroendocrine tumors and overt hypoglycemia was not observed in aged MafA$^{S64F/+}$ female mice (data not shown). Notably, MAFB was recently shown to be essential for the formation of human embryonic-derived β cells and insulin production (Russell et al., 2020), whereas there is no phenotype associated with the loss of MafB in mouse islet β cells except during pregnancy (Cyphert et al., 2019). Thus, we believe that it will be important to extend the analysis of MAFA^{S64F} control to human islets—acutely *in vitro* and chronically after the transplantation of human pseudoislets into immunocompromised mice to directly determine its effect *in vivo*. Such studies should generate keen insight into unique, species-specific, age-dependent, and sex-biased molecular and genetic mechanisms controlling human islet β cell activity.

STAR★METHODS

Detailed methods are provided in the online version of this paper and include the following:

- KEY RESOURCES TABLE

Figure 6. DNA damage and senescence markers are increased in dysfunctional male *MafA*$^{S64F/+}$ islets

(A–C) gH2AX staining (A) and 53BP1 (B), markers of DNA double-strand breaks, and p21, a cell-cycle inhibitor (C), were present in male *MafA*$^{S64F/+}$ (Het) islets. Male *MafA*$^{S64F/+}$ islets had a significant increase in the proportion of islets with >10% p21^{+} cells.

(D) Male *MafA*$^{S64F/+}$ islets showed reduced LaminB1 protein (left) and mRNA (right).

(E and F) SA-β-gal was not produced in 4-week-old male *MafA*$^{S64F/+}$ islets, but was detected in *MafA*$^{S64F/+}$ males by 7 weeks. (E) The SA-β-gal in 7-week-old *MafA*$^{S64F/+}$ islets was of similar intensity to 10- to 12-month-old WT male mouse islets. (F) The proportion of SA-β-gal^{+} islets was quantitated for each sample (n = 3–4). Two-tailed Student t test; **p < 0.01; scale bar, 50 μm.

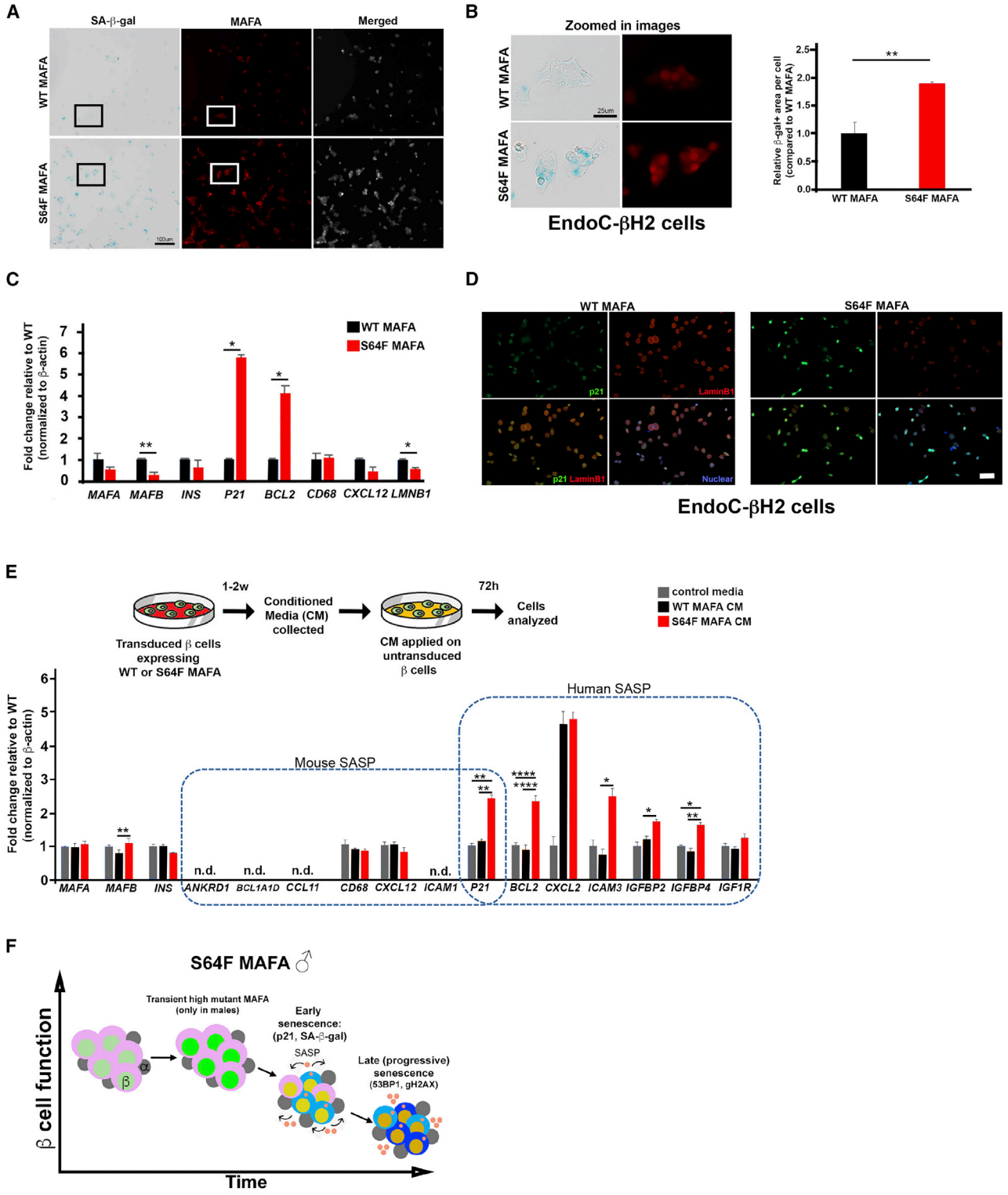

Figure 7. Human β cells expressing MAFA^{S64F} demonstrate accelerated senescence and a species-specific SASP signature

(A) SA-β-gal staining on EndoC-βH2 cells transduced to express WT MAFA or MAFA^{S64F} and stained for MAFA (red). Scale bar, 100 μm.

(B) Inset areas outlined in boxes in (A) are magnified in the left panel. Scale bar, 25 μm. β-gal^{+} area was significantly increased in MAFA^{S64F} cells (right panel).

(C) Human expression of β cell-enriched proteins and senescence associated proteins identified in male *MafA*$^{S64F/+}$ mice. Two-tailed Student t test; *p < 0.05; **p < 0.01.

(legend continued on next page)

- RESOURCE AVAILABILITY
  - Lead contact
  - Materials availability
  - Data and code availability
- EXPERIMENTAL MODEL AND SUBJECT DETAILS
  - Animals
  - Human EndoC-βH2 cells
- METHOD DETAILS
  - Intraperitoneal glucose and insulin tolerance testing
  - Glucose-stimulated hormone secretion
  - Tissue and cell preparation and immunostaining
  - RNA sequencing, analysis, and validation by quantitative real-time PCR
  - Islet cytosolic calcium imaging
  - Senescence-associated β-galactosidase (SA-β-gal) staining
  - Ovariectomy methods
  - Glycogen storage assay
  - Paracrine conditioned media assay
- QUANTIFICATION AND STATISTICAL ANALYSIS

SUPPLEMENTAL INFORMATION

Supplemental information can be found online at https://doi.org/10.1016/j.celrep.2021.109813.

ACKNOWLEDGMENTS

This research was performed using resources and/or funding provided by NIH grants to R.S. (DK090570), E.M.W. (F32 DK109577), J.C. (T32 DK007061), F.M.-J. (DK074970 and DK107444), J.S. (DK109102, HL144846), and D.A.J. (DK097392) and by the Vanderbilt Diabetes Research and Training Center (DK20593). X.T. was supported by a JDRF Fellowship (3-PDF-2019-738-A-N); J.C. by a Doris Duke Charitable Foundation Physician Scientist Fellowship (2020063), and VUMC Harrison Society funds; D.I. by a George Alberti Research Training Fellowship funded by Diabetes UK (16/0005395); and F.M.-J. by a US Department of Veterans Affairs Merit Review Award (BX003725). S.E.F. is supported by a Sir Henry Dale Fellowship jointly sponsored by the Wellcome Trust and the Royal Society (105636/Z/14/Z). We also thank Drs. Raphaël Scharfmann and Phillippe Ravassard for generously providing EndoC-βH2 cells. Imaging was performed with NIH support from the Vanderbilt University Medical Center Cell Imaging Shared Resource (NCI grant CA68485; NIDDK grants DK20593, DK58404, and DK59637; NICHD grant HD15052; and NEI grant EY08126). Islet hormone analysis was performed in the Vanderbilt University Medical Center Islet Procurement and Analysis Core (NIH DK20593) and the Vanderbilt University Neurochemistry Core (NIH U54 HD083211). MafAS64F-expressing mice were produced in the Diabetes Research Center Animal Studies Core at the University of Michigan, which is supported by NIH P30 DK020572.

AUTHOR CONTRIBUTIONS

E.M.W., J.C., X.T., and R.S. designed the initial experiments. E.M.W., J.C., X.T., M.G., and J.-H.L. executed and analyzed the experiments, with input from S.Y., D.I., F.M.-J., S.E.F., M.K., J.S., D.A.J., and R.S. The manuscript was principally written by E.M.W., J.C., X.T., and R.S., although all of the authors have reviewed versions. R.S. is the guarantor of this work and as such had full access to all of the data in the study and takes responsibility for the integrity of the data and the accuracy of the data analysis.

DECLARATION OF INTERESTS

The authors declare no competing interests.

INCLUSION AND DIVERSITY

We worked to ensure sex balance in the selection of non-human subjects. We worked to ensure diversity in experimental samples through the selection of the cell lines. We worked to ensure diversity in experimental samples through the selection of the genomic datasets. While citing references scientifically relevant for this work, we also actively worked to promote gender balance in our reference list. The author list of this paper includes contributors from the location where the research was conducted who participated in the data collection, design, analysis, and/or interpretation of the work.

Received: March 4, 2021
Revised: July 21, 2021
Accepted: September 17, 2021
Published: October 12, 2021

REFERENCES

Aguayo-Mazzucato, C., Koh, A., El Khattabi, I., Li, W.C., Toschi, E., Jermendy, A., Juhl, K., Mao, K., Weir, G.C., Sharma, A., and Bonner-Weir, S. (2011). Mafa expression enhances glucose-responsive insulin secretion in neonatal rat β cells. Diabetologia *54*, 583–593.

Aguayo-Mazzucato, C., Andle, J., Lee, T.B., Jr., Midha, A., Talemal, L., Chipashvili, V., Hollister-Lock, J., van Deursen, J., Weir, G., and Bonner-Weir, S. (2019). Acceleration of β cell aging determines diabetes and senolysis improves disease outcomes. Cell Metab. *30*, 129–142.e4.

Ahlgren, U., Jonsson, J., Jonsson, L., Simu, K., and Edlund, H. (1998). β-cell-specific inactivation of the mouse Ipf1/Pdx1 gene results in loss of the β-cell phenotype and maturity onset diabetes. Genes Dev. *12*, 1763–1768.

Arda, H.E., Li, L., Tsai, J., Torre, E.A., Rosli, Y., Peiris, H., Spitale, R.C., Dai, C., Gu, X., Qu, K., et al. (2016). Age-Dependent Pancreatic Gene Regulation Reveals Mechanisms Governing Human β Cell Function. Cell Metab. *23*, 909–920.

Arrojo E Drigo, R., Lev-Ram, V., Tyagi, S., Ramachandra, R., Deerinck, T., Bushong, E., Phan, S., Orphan, V., Lechene, C., Ellisman, M.H., and Hetzer, M.W. (2019). Age mosaicism across multiple scales in adult tissues. Cell Metab. *30*, 343–351.e3.

Artner, I., Hang, Y., Guo, M., Gu, G., and Stein, R. (2008). MafA is a dedicated activator of the insulin gene in vivo. J. Endocrinol. *198*, 271–279.

Artner, I., Hang, Y., Mazur, M., Yamamoto, T., Guo, M., Lindner, J., Magnuson, M.A., and Stein, R. (2010). MafA and MafB regulate genes critical to β-cells in a unique temporal manner. Diabetes *59*, 2530–2539.

Baker, D.J., Wijshake, T., Tchkonia, T., LeBrasseur, N.K., Childs, B.G., van de Sluis, B., Kirkland, J.L., and van Deursen, J.M. (2011). Clearance of p16Ink4a-

(D) Immunostaining for senescence markers p21 (green) was increased and LaminB1 (red) decreased in MAFA^{S64F}-expressing EndoC-βH2 cells.
(E) CM from WT MAFA or MAFA^{S64F}-expressing EndoC-βH2 cells were collected, purified and added to EndoC-βH2 cells cultured for 72 h. SASP genes upregulated in male *MafA*$^{S64F/+}$ mice were not identified in EndoC-βH2 cells. However, novel, species-specific secretory senescence-associated factors were identified in this context. N.D., not detectable. One-way ANOVA; *$p < 0.05$; **$p < 0.01$; ****$p < 0.0001$.
(F) Schematic of temporal senescence and aging responses in *MafA*^{S64F}-expressing male β cells. In male *MafA*$^{S64F/+}$, transiently high MafA protein triggers molecular insults to induce premature senescence marked by cell-cycle arrest, senescence staining (blue cytoplasmic shade), and initiation of a senescence-associated secretory phenotype (SASP, pink secretory factors), resulting in impaired GSIS. Late (progressive) senescence propagates this phenotype with SASP amplification and diversification.

positive senescent cells delays ageing-associated disorders. Nature *479*, 232–236.

Baker, D.J., Childs, B.G., Durik, M., Wijers, M.E., Sieben, C.J., Zhong, J., Saltness, R.A., Jeganathan, K.B., Verzosa, G.C., Pezeshki, A., et al. (2016). Naturally occurring p16(Ink4a)-positive cells shorten healthy lifespan. Nature *530*, 184–189.

Banerjee, R.R., Cyphert, H.A., Walker, E.M., Chakravarthy, H., Peiris, H., Gu, X., Liu, Y., Conrad, E., Goodrich, L., Stein, R.W., and Kim, S.K. (2016). Gestational Diabetes Mellitus From Inactivation of Prolactin Receptor and MafB in Islet β-Cells. Diabetes *65*, 2331–2341.

Barbetti, F., and D'Annunzio, G. (2018). Genetic causes and treatment of neonatal diabetes and early childhood diabetes. Best Pract. Res. Clin. Endocrinol. Metab. *32*, 575–591.

Basisty, N., Meyer, J.G., and Schilling, B. (2018). Protein Turnover in Aging and Longevity. Proteomics *18*, e1700108.

Bergsten, P., Grapengiesser, E., Gylfe, E., Tengholm, A., and Hellman, B. (1994). Synchronous oscillations of cytoplasmic Ca2+ and insulin release in glucose-stimulated pancreatic islets. J. Biol. Chem. *269*, 8749–8753.

Blum, B., Roose, A.N., Barrandon, O., Maehr, R., Arvanites, A.C., Davidow, L.S., Davis, J.C., Peterson, Q.P., Rubin, L.L., and Melton, D.A. (2014). Reversal of β cell de-differentiation by a small molecule inhibitor of the TGFβ pathway. eLife *3*, e02809.

Bosco, D., Armanet, M., Morel, P., Niclauss, N., Sgroi, A., Muller, Y.D., Giovannoni, L., Parnaud, G., and Berney, T. (2010). Unique arrangement of α- and β-cells in human islets of Langerhans. Diabetes *59*, 1202–1210.

Brissova, M., Fowler, M.J., Nicholson, W.E., Chu, A., Hirshberg, B., Harlan, D.M., and Powers, A.C. (2005). Assessment of human pancreatic islet architecture and composition by laser scanning confocal microscopy. J. Histochem. Cytochem. *53*, 1087–1097.

Butler, P.C., Meier, J.J., Butler, A.E., and Bhushan, A. (2007). The replication of β cells in normal physiology, in disease and for therapy. Nat. Clin. Pract. Endocrinol. Metab. *3*, 758–768.

Cabrera, O., Berman, D.M., Kenyon, N.S., Ricordi, C., Berggren, P.O., and Caicedo, A. (2006). The unique cytoarchitecture of human pancreatic islets has implications for islet cell function. Proc. Natl. Acad. Sci. USA *103*, 2334–2339.

Campisi, J. (2014). Cell biology: the beginning of the end. Nature *505*, 35–36.

Campisi, J., and d'Adda di Fagagna, F. (2007). Cellular senescence: when bad things happen to good cells. Nat. Rev. Mol. Cell Biol. *8*, 729–740.

Camunas-Soler, J., Dai, X., Hang, Y., Bautista, A., Lyon, J., Suzuki, K., Kim, S., Quake, S., and MacDonald, P. (2020). Patch-Seq links single-cell transcriptomes to human islet dysfunction in diabets. Cell Metab. *5*, 1017–1031.

Chang, J., Wang, Y., Shao, L., Laberge, R.M., Demaria, M., Campisi, J., Janakiraman, K., Sharpless, N.E., Ding, S., Feng, W., et al. (2016). Clearance of senescent cells by ABT263 rejuvenates aged hematopoietic stem cells in mice. Nat. Med. *22*, 78–83.

Chen, C., Shiota, C., Agostinelli, G., Ridley, D., Jiang, Y., Ma, J., Prasadan, K., Xiao, X., and Gittes, G.K. (2019). Evidence of a developmental origin for β-cell heterogeneity using a dual lineage-tracing technology. Development *146*, dev164913.

Childs, B.G., Baker, D.J., Wijshake, T., Conover, C.A., Campisi, J., and van Deursen, J.M. (2016). Senescent intimal foam cells are deleterious at all stages of atherosclerosis. Science *354*, 472–477.

Conrad, E., Dai, C., Spaeth, J., Guo, M., Cyphert, H.A., Scoville, D., Carroll, J., Yu, W.M., Goodrich, L.V., Harlan, D.M., et al. (2016). The MAFB transcription factor impacts islet α-cell function in rodents and represents a unique signature of primate islet β-cells. Am. J. Physiol. Endocrinol. Metab. *310*, E91–E102.

Coppé, J.P., Desprez, P.Y., Krtolica, A., and Campisi, J. (2010). The senescence-associated secretory phenotype: the dark side of tumor suppression. Annu. Rev. Pathol. *5*, 99–118.

Cyphert, H.A., Walker, E.M., Hang, Y., Dhawan, S., Haliyur, R., Bonatakis, L., Avrahami, D., Brissova, M., Kaestner, K.H., Bhushan, A., et al. (2019). Examining how the MAFB transcription factor affects islet β cell function postnatally. Diabetes *68*, 337–348.

Dadi, P.K., Luo, B., Vierra, N.C., and Jacobson, D.A. (2015). TASK-1 Potassium Channels Limit Pancreatic α-Cell Calcium Influx and Glucagon Secretion. Mol. Endocrinol. *29*, 777–787.

Dai, C., Brissova, M., Hang, Y., Thompson, C., Poffenberger, G., Shostak, A., Chen, Z., Stein, R., and Powers, A.C. (2012). Islet-enriched gene expression and glucose-induced insulin secretion in human and mouse islets. Diabetologia *55*, 707–718.

Fang, L., Igarashi, M., Leung, J., Sugrue, M.M., Lee, S.W., and Aaronson, S.A. (1999). p21Waf1/Cip1/Sdi1 induces permanent growth arrest with markers of replicative senescence in human tumor cells lacking functional p53. Oncogene *18*, 2789–2797.

Fiaschi-Taesch, N.M., Salim, F., Kleinberger, J., Troxell, R., Cozar-Castellano, I., Selk, K., Cherok, E., Takane, K.K., Scott, D.K., and Stewart, A.F. (2010). Induction of human β-cell proliferation and engraftment using a single G1/S regulatory molecule, cdk6. Diabetes *59*, 1926–1936.

Franceschi, C., Garagnani, P., Parini, P., Giuliani, C., and Santoro, A. (2018). Inflammaging: a new immune-metabolic viewpoint for age-related diseases. Nat. Rev. Endocrinol. *14*, 576–590.

Franklin, I., Gromada, J., Gjinovci, A., Theander, S., and Wollheim, C.B. (2005). Beta-cell secretory products activate alpha-cell ATP-dependent potassium channels to inhibit glucagon release. Diabetes *54*, 1808–1815.

Freund, A., Laberge, R.M., Demaria, M., and Campisi, J. (2012). Lamin B1 loss is a senescence-associated biomarker. Mol. Biol. Cell *23*, 2066–2075.

Gale, E.A. (2002). Can we change the course of beta-cell destruction in type 1 diabetes? N. Engl. J. Med. *346*, 1740–1742.

Gannon, M., Kulkarni, R.N., Tse, H.M., and Mauvais-Jarvis, F. (2018). Sex differences underlying pancreatic islet biology and its dysfunction. Mol. Metab. *15*, 82–91.

Gilbert, J.M., and Blum, B. (2018). Synaptotagmins Tweak Functional β Cell Maturation. Dev. Cell *45*, 284–286.

Golson, M.L., and Kaestner, K.H. (2017). Epigenetics in formation, function, and failure of the endocrine pancreas. Mol. Metab. *6*, 1066–1076.

Gorgoulis, V., Adams, P.D., Alimonti, A., Bennett, D.C., Bischof, O., Bishop, C., Campisi, J., Collado, M., Evangelou, K., Ferbeyre, G., et al. (2019). Cellular Senescence: Defining a Path Forward. Cell *179*, 813–827.

Greenhill, C. (2019). Regulating metabolism and ageing - the role of PI3K. Nat. Rev. Endocrinol. *15*, 376–377.

Guo, S., Burnette, R., Zhao, L., Vanderford, N.L., Poitout, V., Hagman, D.K., Henderson, E., Ozcan, S., Wadzinski, B.E., and Stein, R. (2009). The stability and transactivation potential of the mammalian MafA transcription factor are regulated by serine 65 phosphorylation. J. Biol. Chem. *284*, 759–765.

Guo, S., Vanderford, N.L., and Stein, R. (2010). Phosphorylation within the MafA N terminus regulates C-terminal dimerization and DNA binding. J. Biol. Chem. *285*, 12655–12661.

Guo, S., Dai, C., Guo, M., Taylor, B., Harmon, J.S., Sander, M., Robertson, R.P., Powers, A.C., and Stein, R. (2013). Inactivation of specific β cell transcription factors in type 2 diabetes. J. Clin. Invest. *123*, 3305–3316.

Han, S.I., Aramata, S., Yasuda, K., and Kataoka, K. (2007). MafA stability in pancreatic β cells is regulated by glucose and is dependent on its constitutive phosphorylation at multiple sites by glycogen synthase kinase 3. Mol. Cell. Biol. *27*, 6593–6605.

Hang, Y., and Stein, R. (2011). MafA and MafB activity in pancreatic β cells. Trends Endocrinol. Metab. *22*, 364–373.

Hang, Y., Yamamoto, T., Benninger, R.K., Brissova, M., Guo, M., Bush, W., Piston, D.W., Powers, A.C., Magnuson, M., Thurmond, D.C., and Stein, R. (2014). The MafA transcription factor becomes essential to islet β-cells soon after birth. Diabetes *63*, 1994–2005.

Harmon, J.S., Stein, R., and Robertson, R.P. (2005). Oxidative stress-mediated, post-translational loss of MafA protein as a contributing mechanism to loss of insulin gene expression in glucotoxic beta cells. J. Biol. Chem. *280*, 11107–11113.

Helman, A., Klochendler, A., Azazmeh, N., Gabai, Y., Horwitz, E., Anzi, S., Swisa, A., Condiotti, R., Granit, R.Z., Nevo, Y., et al. (2016). p16(Ink4a)-induced senescence of pancreatic beta cells enhances insulin secretion. Nat. Med. *22*, 412–420.

Henquin, J.C., Dufrane, D., and Nenquin, M. (2006). Nutrient control of insulin secretion in isolated normal human islets. Diabetes *55*, 3470–3477.

Herranz, N., and Gil, J. (2018). Mechanisms and functions of cellular senescence. J. Clin. Invest. *128*, 1238–1246.

Iacovazzo, D., Flanagan, S.E., Walker, E., Quezado, R., de Sousa Barros, F.A., Caswell, R., Johnson, M.B., Wakeling, M., Brändle, M., Guo, M., et al. (2018). *MAFA* missense mutation causes familial insulinomatosis and diabetes mellitus. Proc. Natl. Acad. Sci. USA *115*, 1027–1032.

Jacobson, D.A., and Shyng, S.L. (2020). Ion Channels of the Islets in Type 2 Diabetes. J. Mol. Biol. *432*, 1326–1346.

Kabir, T.D., Leigh, R.J., Tasena, H., Mellone, M., Coletta, R.D., Parkinson, E.K., Prime, S.S., Thomas, G.J., Paterson, I.C., Zhou, D., et al. (2016). A miR-335/COX-2/PTEN axis regulates the secretory phenotype of senescent cancer-associated fibroblasts. Aging (Albany NY) *8*, 1608–1635.

Kalwat, M.A., and Cobb, M.H. (2017). Mechanisms of the amplifying pathway of insulin secretion in the β cell. Pharmacol. Ther. *179*, 17–30.

Kurz, D.J., Decary, S., Hong, Y., and Erusalimsky, J.D. (2000). Senescence-associated (beta)-galactosidase reflects an increase in lysosomal mass during replicative ageing of human endothelial cells. J. Cell Sci. *113*, 3613–3622.

Lecoin, L., Rocques, N., El-Yakoubi, W., Ben Achour, S., Larcher, M., Pouponnot, C., and Eychène, A. (2010). MafA transcription factor identifies the early ret-expressing sensory neurons. Dev. Neurobiol. *70*, 485–497.

Love, M.I., Huber, W., and Anders, S. (2014). Moderated estimation of fold change and dispersion for RNA-seq data with DESeq2. Genome Biol. *15*, 550.

Luan, C., Ye, Y., Singh, T., Barghouth, M., Eliasson, L., Artner, I., Zhang, E., and Renström, E. (2019). The calcium channel subunit gamma-4 is regulated by MafA and necessary for pancreatic beta-cell specification. Commun. Biol. *2*, 106.

Madsen, O.D., Jensen, J., Petersen, H.V., Pedersen, E.E., Oster, A., Andersen, F.G., Jørgensen, M.C., Jensen, P.B., Larsson, L.I., and Serup, P. (1997). Transcription factors contributing to the pancreatic beta-cell phenotype. Horm. Metab. Res. *29*, 265–270.

Mancini, M., Saintigny, G., Mahé, C., Annicchiarico-Petruzzelli, M., Melino, G., and Candi, E. (2012). MicroRNA-152 and -181a participate in human dermal fibroblasts senescence acting on cell adhesion and remodeling of the extracellular matrix. Aging (Albany NY) *4*, 843–853.

Martin, N., and Bernard, D. (2018). Calcium signaling and cellular senescence. Cell Calcium *70*, 16–23.

Martinez, M.N., Emfinger, C.H., Overton, M., Hill, S., Ramaswamy, T.S., Cappel, D.A., Wu, K., Fazio, S., McDonald, W.H., Hachey, D.L., et al. (2012). Obesity and altered glucose metabolism impact HDL composition in CETP transgenic mice: a role for ovarian hormones. J. Lipid Res. *53*, 379–389.

Niceta, M., Stellacci, E., Gripp, K.W., Zampino, G., Kousi, M., Anselmi, M., Traversa, A., Ciolfi, A., Stabley, D., Bruselles, A., et al. (2015). Mutations Impairing GSK3-Mediated MAF Phosphorylation Cause Cataract, Deafness, Intellectual Disability, Seizures, and a Down Syndrome-like Facies. Am. J. Hum. Genet. *96*, 816–825.

Pan, F.C., and Wright, C. (2011). Pancreas organogenesis: from bud to plexus to gland. Dev. Dyn. *240*, 530–565.

Pan, F.C., Brissova, M., Powers, A.C., Pfaff, S., and Wright, C.V. (2015). Inactivating the permanent neonatal diabetes gene Mnx1 switches insulin-producing β-cells to a δ-like fate and reveals a facultative proliferative capacity in aged β-cells. Development *142*, 3637–3648.

Raum, J.C., Gerrish, K., Artner, I., Henderson, E., Guo, M., Sussel, L., Schisler, J.C., Newgard, C.B., and Stein, R. (2006). FoxA2, Nkx2.2, and PDX-1 regulate islet beta-cell-specific mafA expression through conserved sequences located between base pairs -8118 and -7750 upstream from the transcription start site. Mol. Cell. Biol. *26*, 5735–5743.

Raum, J.C., Hunter, C.S., Artner, I., Henderson, E., Guo, M., Elghazi, L., Sosa-Pineda, B., Ogihara, T., Mirmira, R.G., Sussel, L., and Stein, R. (2010). Islet beta-cell-specific MafA transcription requires the 5′-flanking conserved region 3 control domain. Mol. Cell. Biol. *30*, 4234–4244.

Rocques, N., Abou Zeid, N., Sii-Felice, K., Lecoin, L., Felder-Schmittbuhl, M.P., Eychène, A., and Pouponnot, C. (2007). GSK-3-mediated phosphorylation enhances Maf-transforming activity. Mol. Cell *28*, 584–597.

Russell, R., Carnese, P.P., Hennings, T.G., Walker, E.M., Russ, H.A., Liu, J.S., Giacometti, S., Stein, R., and Hebrok, M. (2020). Loss of the transcription factor MAFB limits β-cell derivation from human PSCs. Nat. Commun. *11*, 2742.

Sampathkumar, N.K., Bravo, J.I., Chen, Y., Danthi, P.S., Donahue, E.K., Lai, R.W., Lu, R., Randall, L.T., Vinson, N., and Benayoun, B.A. (2020). Widespread sex dimorphism in aging and age-related diseases. Hum. Genet. *139*, 333–356.

Scharfmann, R., Pechberty, S., Hazhouz, Y., von Bülow, M., Bricout-Neveu, E., Grenier-Godard, M., Guez, F., Rachdi, L., Lohmann, M., Czernichow, P., and Ravassard, P. (2014). Development of a conditionally immortalized human pancreatic β cell line. J. Clin. Invest. *124*, 2087–2098.

Schultz, L.B., Chehab, N.H., Malikzay, A., and Halazonetis, T.D. (2000). p53 binding protein 1 (53BP1) is an early participant in the cellular response to DNA double-strand breaks. J. Cell Biol. *151*, 1381–1390.

Scoville, D.W., Cyphert, H.A., Liao, L., Xu, J., Reynolds, A., Guo, S., and Stein, R. (2015). MLL3 and MLL4 methyltransferases bind to the MAFA and MAFB transcription factors to regulate islet β cell function. Diabetes *64*, 3772–3783.

Shih, H.P., Wang, A., and Sander, M. (2013). Pancreas organogenesis: from lineage determination to morphogenesis. Annu. Rev. Cell Dev. Biol. *29*, 81–105.

Thompson, P.J., Shah, A., Ntranos, V., Van Gool, F., Atkinson, M., and Bhushan, A. (2019). Targeted elimination of senescent beta cells prevents type 1 diabetes. Cell Metab. *29*, 1045–1060.e10.

Tyrberg, B., Andersson, A., and Borg, L.A. (2001). Species differences in susceptibility of transplanted and cultured pancreatic islets to the beta-cell toxin alloxan. Gen. Comp. Endocrinol. *122*, 238–251.

van der Meulen, T., Donaldson, C.J., Cáceres, E., Hunter, A.E., Cowing-Zitron, C., Pound, L.D., Adams, M.W., Zembrzycki, A., Grove, K.L., and Huising, M.O. (2015). Urocortin3 mediates somatostatin-dependent negative feedback control of insulin secretion. Nat. Med. *21*, 769–776.

van Deursen, J.M. (2014). The role of senescent cells in ageing. Nature *509*, 439–446.

Walker, J.T., Haliyur, R., Nelson, H.A., Ishahak, M., Poffenberger, G., Aramandla, R., Reihsmann, C., Luchsinger, J.R., Saunders, D.C., Wang, P., et al. (2020). Integrated human pseudoislet system and microfluidic platform demonstrate differences in GPCR signaling in islet cells. JCI Insight *5*, e137017.

Zhang, C., Moriguchi, T., Kajihara, M., Esaki, R., Harada, A., Shimohata, H., Oishi, H., Hamada, M., Morito, N., Hasegawa, K., et al. (2005). MafA is a key regulator of glucose-stimulated insulin secretion. Mol. Cell. Biol. *25*, 4969–4976.

STAR★METHODS

KEY RESOURCES TABLE

REAGENT or RESOURCE	SOURCE	IDENTIFIER
Antibodies		
Guinea pig anti-Insulin	Thermo Fisher	Cat#PA1 26938; RRID:AB_794668
Mouse anti-Glucagon	Sigma	Cat#G2654; RRID:AB_259852
Mouse anti-Ki67	BD Biosciences	Cat#550609; RRID:AB_393778
DAPI Fluoromount-G mounting medium	SouthernBiotech	Cat#0100-20
Rabbit anti-MAFA	Cell Signaling	Cat#79737; RRID:AB_2799938
Goat anti-PDX-1	Chris Wright, Vanderbilt	N/A
Rabbit anti-UCN3	Phoenix	Cat#H-019-028; RRID:AB_2889826
Goat anti-P21 (for cells)	Santa Cruz	Cat#sc-397G; RRID:AB_632127
Rat anti-P21 (for tissue sections)	Abcam	Cat#ab107099; RRID:AB_10891759
Rabbit anti-53BP1	Bethyl	Cat#A300-272A; RRID:AB_185520
Rabbit anti-gH2AX	Abcam	Cat#ab81299; RRID:AB_1640564
Rabbit anti-LaminB1	Abcam	Cat#16048; RRID:AB_443298
Bacterial and virus strains		
Lentivirus: $MAFA^{WT}$-pCDH-EF1-MCS-IRES-GopGFP	Modified for this paper from System Biosciences	Cat#CD521A-1
Lentivirus: $MAFA^{S64F}$-pCDH-EF1-MCS-IRES-GopGFP	Modified for this paper from System Biosciences	Cat#CD521A-1
Chemicals, peptides, and recombinant proteins		
Fura-2 AM	Life Technologies	Cat#F1221
Critical commercial assays		
Cell Death Detection Kit	Roche	Cat#11684795910
Senescence β-Galactosidase Staining Kit	Cell Signaling	Cat#9860
Glycogen Assay Kit	Cayman Chemicals	Cat#700480
Deposited data		
Raw and analyzed data	This paper	GEO:GSE183561
Experimental models: Cell lines		
Human: EndoC-βH2 Cells	Scharfmann et al., 2014	N/A
Experimental models: Organisms/strains		
Mouse: *MafA*$^{S64F/+}$	This paper	N/A
Oligonucleotides		
Primers for mouse and human see Table S1	This paper	N/A
Software and algorithms		
Genialis visual informatics platform: BBDuk, START aligner, featureCounts	https://www.genialis.com	N/A
DESeq2	Love et al., 2014	N/A
ImageJ	https://imagej.nih.gov/ij/	N/A
ImageScope Software	Aperio Technologies	N/A

RESOURCE AVAILABILITY

Lead contact

Further information and requests for resources and reagents should be directed to and will be fulfilled by the lead contact, Roland Stein (roland.stein@vanderbilt.edu).

Materials availability

All unique/stable reagents generated in this study are available from the lead contact with a completed materials transfer agreement.

Data and code availability

- All data needed to evaluate the conclusions in the paper are present in the paper and/or the Supplemental information. Bulk RNA-seq data have been deposited to GEO and are publicly available at the date of publication. Accession number is listed in the Key resources table.
- This paper does not report original code.
- Any additional information required to reanalyze the data reported in this work paper is available from the Lead Contact upon request.

EXPERIMENTAL MODEL AND SUBJECT DETAILS

Animals

S64F MafA-expressing mice were generated using CRISPR/Cas9 targeting by the University of Michigan Transgenic Core in the C57BL/6J mouse strain. Viable animals and progeny were screened for the appropriate mutation by DNA sequencing (Molecular Resource Center, University of Tennessee Health Science Center). Wild-type (WT) littermates were used as controls. *MafA*$^{S64F/+}$ were born at normal Mendelian ratios while homozygous *MafA*$^{S64F/S64F}$ variants were not (see Figure S2). Mice of both sexes were used in this study; details can be found in the results section and figure legends. All animal studies were reviewed and approved by the Vanderbilt University Institutional Animal Care and Use Committee. Mice were housed and cared for according to the Vanderbilt Department of Animal Care and the Institutional Animal Care and Use Committee of Animal Welfare Assurance Standards and Guidelines.

Human EndoC-βH2 cells

Human EndoC-βH2 cells were grown in DMEM containing 5.6mM glucose, 2% BSA, 50 μM 2-mercaptoethanol, 10mM nicotinamide, 5.5 μg/mL transferrin, 6.7 ng/mL selenite, 100 units/mL penicillin, and 100 units/mL streptomycin (Scharfmann et al., 2014). For gene transfection, cells were incubated with lentiviral particles (150ng for cells cultured in a 6cm dish) containing either MAFA^{WT}-expressing or MAFA^{S64F}-expressing sequences one day after plating. Assays were performed one week following infection unless specified otherwise.

METHOD DETAILS

Intraperitoneal glucose and insulin tolerance testing

Glucose tolerance testing was performed on WT and *MafA*$^{S64F/+}$ mice (n = 4-16) given an intraperitoneal injection of D-glucose (2 mg/g body weight) prepared in sterile PBS (20% w/v) after a 6-hour fast. Insulin tolerance tests were conducted by intraperitoneal injection of 0.5 IU/kg body weight insulin (Novolin, regular human insulin, recombinant DNA origin) into mice (n = 3-5) fasted for 6 hours. Blood glucose was measured using a FreeStyle glucometer (Abbott Diabetes Care) before (0 minutes) and at 15, 30, 60, and 120 minutes following injection. Serum insulin was measured by radioimmunoassay at the Vanderbilt Hormone Assay and Analytical Services Core using blood collected following the 6-hour fast. Serum testosterone was measured by the University of Virginia Center for Research in Reproduction Ligand Assay and Analysis Core.

Glucose-stimulated hormone secretion

WT and *MafA*$^{S64F/+}$ mouse (n = 3-6) islets were isolated using standard islet isolation conditions, and hormone secretion was assessed as described previously (Cyphert et al., 2019). The outcome was presented as secreted insulin or glucagon relative to the total islet DNA content (ng/μg DNA (insulin) or pg/μg DNA (glucagon)). Islet hormone content was presented as the concentration of insulin or glucagon per DNA content (Quant-iT PicoGreen, Invitrogen) in each reaction (ng/ng DNA).

For perifusion analysis, islets from 8-10 week old female and male WT and *MafA*$^{S64F/+}$ mice were studied in a dynamic cell perifusion system at a perifusate flow rate of 1 mL/min (Walker et al., 2020) in the Vanderbilt Islet Procurement and Analysis Core. The effluent was collected at 3-minute intervals using an automatic fraction collector. The insulin concentration in each perifusion fraction and islet extract was measured by radioimmunoassay (Millipore).

Tissue and cell preparation and immunostaining

For immunostaining, WT and *MafA*$^{S64F/+}$ pancreata were fixed in 4% (v/v) paraformaldehyde, embedded in either Tissue-Plus O.C.T. (Thermo Fisher Scientific) or paraffin wax, and sectioned to 6 μm thickness. Immunofluorescent images were obtained using a Zeiss Axio Imager M2 widefield microscope with ApoTome. Immunofluorescence staining was performed as previously described with the antibodies listed in Key resources table. Islet β- and α- cell areas were determined as described previously (Cyphert et al., 2019). Briefly, pancreatic sections taken every 50 μm (n = 3-4 animals per genotype) were scanned using a ScanScope CS scanner (Aperio

Technologies, Vista, CA). Images from each experiment were processed with ImageScope Software (Aperio Technologies, Vista, CA). Islet β- and α-cell areas were calculated as the ratio of the insulin- or glucagon-positive area to total pancreas area (eosin stained). The TUNEL assay was performed using an *in situ* cell death detection kit (Roche, #11684795910). In EndoC-βH2 cells, immunostaining for LaminB1, 53BP1, and p21 were also performed (see Key resources table).

RNA sequencing, analysis, and validation by quantitative real-time PCR

RNA was isolated from WT and *MafA*$^{S64F/+}$ islets (n = 4 each for males, n = 5 each for females) using the RNAqueous total RNA isolation kit (Ambion; Thermo Fisher), and then analyzed on an Agilent 2100 Bioanalyzer. Only samples with an RNA Integrity Number > 8.0 were used for library preparation. cDNA libraries were constructed and paired-end sequencing of 4-5 replicates was performed on an Illumina NovaSeq6000 (150 nucleotide reads). The generated FASTQ files were processed and interpreted using the Genialis visual informatics platform (https://www.genialis.com). Reads were preprocessed by BBDuk which removes adapters, trims reads for quality from the 3′ end, and discards reads that are too short after trimming. Preprocessed reads were aligned by START aligner and quantification was done using featureCounts. FastQC reports, alignment statistics and rRNA/globin depletion rate QC information is automatically summarized by the MultiQC tool. Differential gene expression analyses were performed with DESeq2 (Love et al., 2014) with a log2(fold change) threshold of 1 and FDR < 0.05 using the genome build GRCm38. Tab-delimited text files include FPKM values for each sample.

Quantitative real-time PCR expression analysis of selected candidates were performed on independently isolated mouse islets and EndoC-βH2 cells. Trizol reagent (Life Technologies) was used to collect RNA. The cDNAs produced from the iScript cDNA Synthesis Kit (Bio-Rad) were processed in a LightCycler 480 II system (Roche), and analyzed by the ΔΔCT method with primers provided in Key resources table. Significance was calculated by comparing the ΔCT values.

Islet cytosolic calcium imaging

Approximately 60 WT and *MafA*$^{S64F/+}$ islets from at least 6 female and male mice were analyzed with the ratiometric calcium indicator fura-2-acetoxymethylester (Fura-2 AM) (Life Technologies). Islets were maintained in 5 mM glucose culture media for 30 min prior to being loaded with 2 μM Fura-2 AM for 20 min, washed, transferred to a hand-made agarose gel small-volume chamber in a glass bottom dish filled with regular HBSS (5 mM glucose, Thermo Fisher). The 11 mM glucose-induced calcium oscillations and depolarization-activated calcium influx at 30 mM KCl were measured. Images were taken using a Nikon Eclipse TE2000-U microscope equipped with an epifluorescence illuminator (SUTTER, Inc), a CCD camera (HQ2; Photometrics, Inc), and Nikon Elements software (NIKON, Inc) as described before (Dadi et al., 2015).

Senescence-associated β-galactosidase (SA-β-gal) staining

WT and *MafA*$^{S64F/+}$ pancreata were snap frozen in O.C.T. and cryosections were prepared at 16 μm thickness. SA-β-gal activity staining was performed at pH 6.0 (Kurz et al., 2000) using a commercial kit (Cell Signaling, #9860). To compare the intensity of SA-β-gal staining, sections from different genotypes and ages were processed on the same slide. Staining reactions were developed for 18 hours at 37°C, then stopped by 3x PBS washes (pH 7.4). Slides were then subject to immunostaining for insulin by fixing in 4% paraformaldehyde for 45 minutes, permeabilized with Tris-buffered saline with 0.2% Triton X-100 for 15 minutes, blocked in 2% normal donkey serum/1% BSA in PBS and incubated overnight with guinea pig anti-insulin (1:500, Abcam) at 4°C. HRP-conjugated secondary antibodies were incubated on slides for 1 hour and detected with the DAB+ chromogen kit (DAKO). After washing, slides were mounted and imaged by brightfield microscopy. The total number of SA-β-gal^{+} islets per pancreas section were analyzed on ImageJ.

The same kit and condition were also used to evaluate the SA-β-gal activity in EndoC-βH2 cells cultured on chamber slides from different conditions. Staining reactions were stopped after developing for 2 to 3 hours at 37°C with 3x PBS washes (pH 7.4). Slides were then subject to immunostaining for MAFA by fixing in 4% paraformaldehyde for 12 minutes, permeabilized with Tris-buffered saline with 0.5% Triton X-100 for 5 minutes, blocked in 2% normal donkey serum/1% BSA in PBS and incubated overnight with Rabbit α-MAFA (1:500, Novus (NBP1-00121) at 4°C. After washing, slides were mounted and imaged on a Zeiss Axio Imager M2 widefield microscope with ApoTome. Average SA-β-gal+ area/cell was analyzed on ImageJ.

Ovariectomy methods

WT and *MafA*$^{S64F/+}$ female mice underwent ovariectomy at 3 weeks to remove the contribution of endogenous ovarian hormones and prevent completion of sexual maturity (Martinez et al., 2012). Mice were anesthetized with 1%–5% inhaled isoflurane, and placed prone on a heating pad to maintain their body temperature at 37°C. The mice received subcutaneous ketofen at 5-10 mg/kg prior to surgery and post-operatively for two days for pain relief. Intraperitoneal ceftriaxone at 20-40 mg/kg was given once intraoperatively for infection prophylaxis. After adequate anesthesia and analgesia, a midline 1.5 cm incision was made along the shaved mid-dorsal surface of the mouse. Within the retroperitoneal cavity, the ovaries were located and ligated. The incision was closed using surgical staples, which were removed on post-operative day three. Mice were housed singly during recovery and regrouped post-operatively.

Glycogen storage assay

Liver and gastrocnemius muscle from WT and *MafA*$^{S64F/+}$ mice (n = 5 per genotype and sex) were collected and flash frozen in liquid nitrogen. Tissue was homogenized with a Dounce homogenizer prior to determining glycogen content using a glycogen assay kit (Cayman Chemical) according to the manufacturer's protocol.

Paracrine conditioned media assay

Conditioned media (CM) produced after 24 hours of culture from $MAFA^{S64F}$- and $MAFA^{WT}$-expressing human EndoC-βH2 cells were clarified by centrifugation at 500xg for 5 minutes and then at 3000xg for 5 minutes. CM was stored at 4°C for up to 3 weeks prior to use. EndoC-βH2 cells plated on 12-well plate were cultured with a 1:1 mix of EndoC-βH2 islet media (4% BSA) and albumin-free CM collected from $MAFA^{WT}$ or $MAFA^{S64F}$ expressing cells (resulting in 2% BSA in the final medium). For controls, EndoC-βH2 cells from the same passage were cultured in a 1:1 mix of regular EndoC-βH2 cells media and albumin-free media alone (not conditioned by cells), also resulting in 2% BSA in the final medium. After 72 hours, EndoC-βH2 cells were harvested for analysis.

QUANTIFICATION AND STATISTICAL ANALYSIS

Statistical significance was determined using the two-tailed Student t test, one-way ANOVA or two-way ANOVA and Tukey post hoc test as indicated in the figure legends. Data are presented as the mean ± SEM. A threshold of at least $p < 0.05$ was used to declare significance.

Cell Reports, Volume *37*

Supplemental information

Sex-biased islet β cell dysfunction is caused by the MODY MAFA S64F variant by inducing premature aging and senescence in males

Emily M. Walker, Jeeyeon Cha, Xin Tong, Min Guo, Jin-Hua Liu, Sophia Yu, Donato Iacovazzo, Franck Mauvais-Jarvis, Sarah E. Flanagan, Márta Korbonits, John Stafford, David A. Jacobson, and Roland Stein

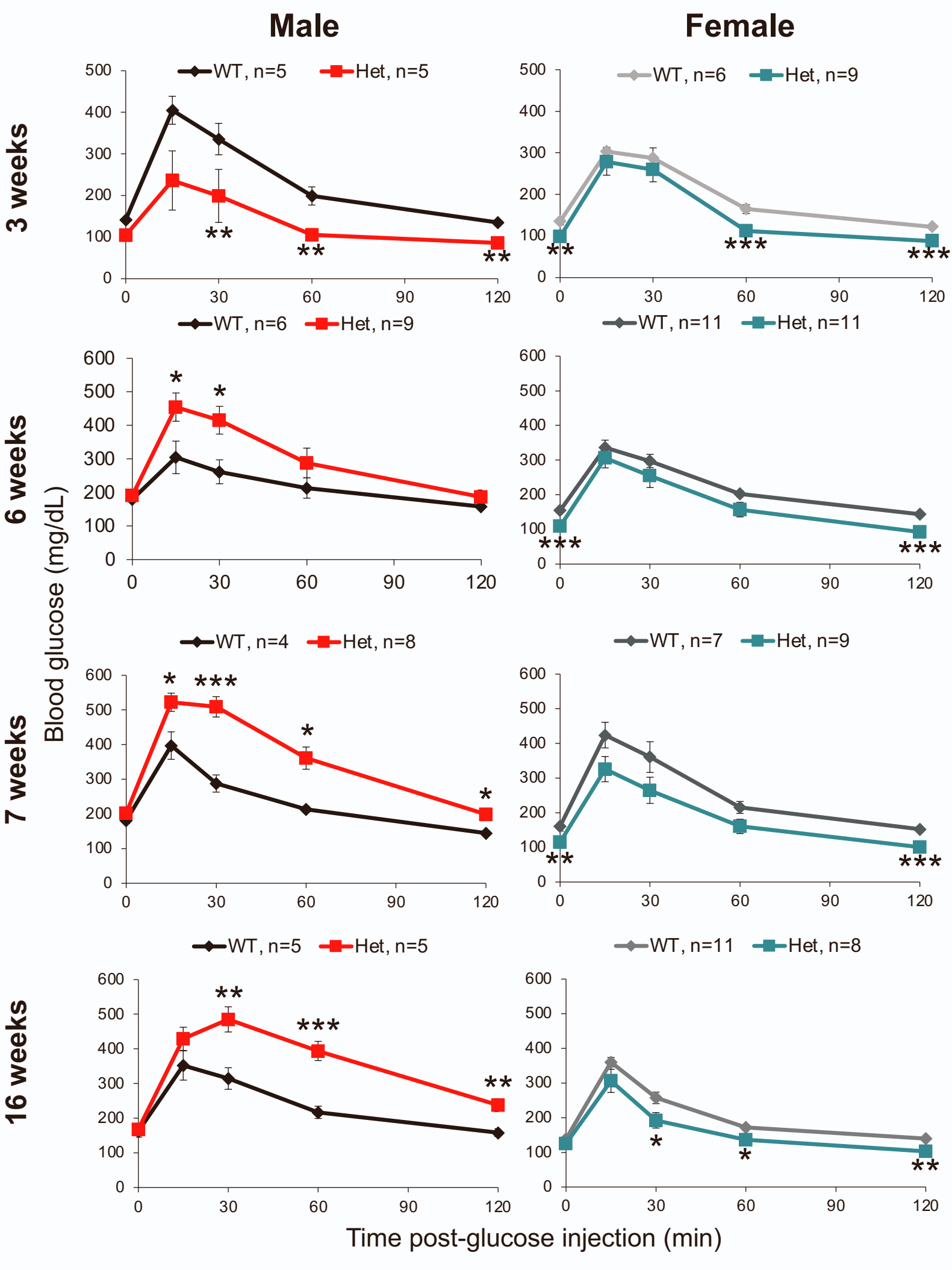
Male
Female
3 weeks
6 weeks
7 weeks
16 weeks
WT, n=5
Het, n=5
WT, n=6
Het, n=9
WT, n=6
Het, n=9
WT, n=11
Het, n=11
WT, n=4
Het, n=8
WT, n=7
Het, n=9
WT, n=5
Het, n=5
WT, n=11
Het, n=8
Blood glucose (mg/dL)
Time post-glucose injection (min)

Figure S1: Glucose tolerance phenotypes were stably maintained in male and female *MafA*$^{S64F/+}$ mice. Related to Figure 1. GTT was performed in 3-, 6-, 7-, and 16-week-old mice. Glucose (2mg/kg) was injected following a 6 hour fast and blood glucose was measured at the indicated time points. Two-tail Student *t* test; *p<0.05; **p<0.01; ***p<0.001.

a)

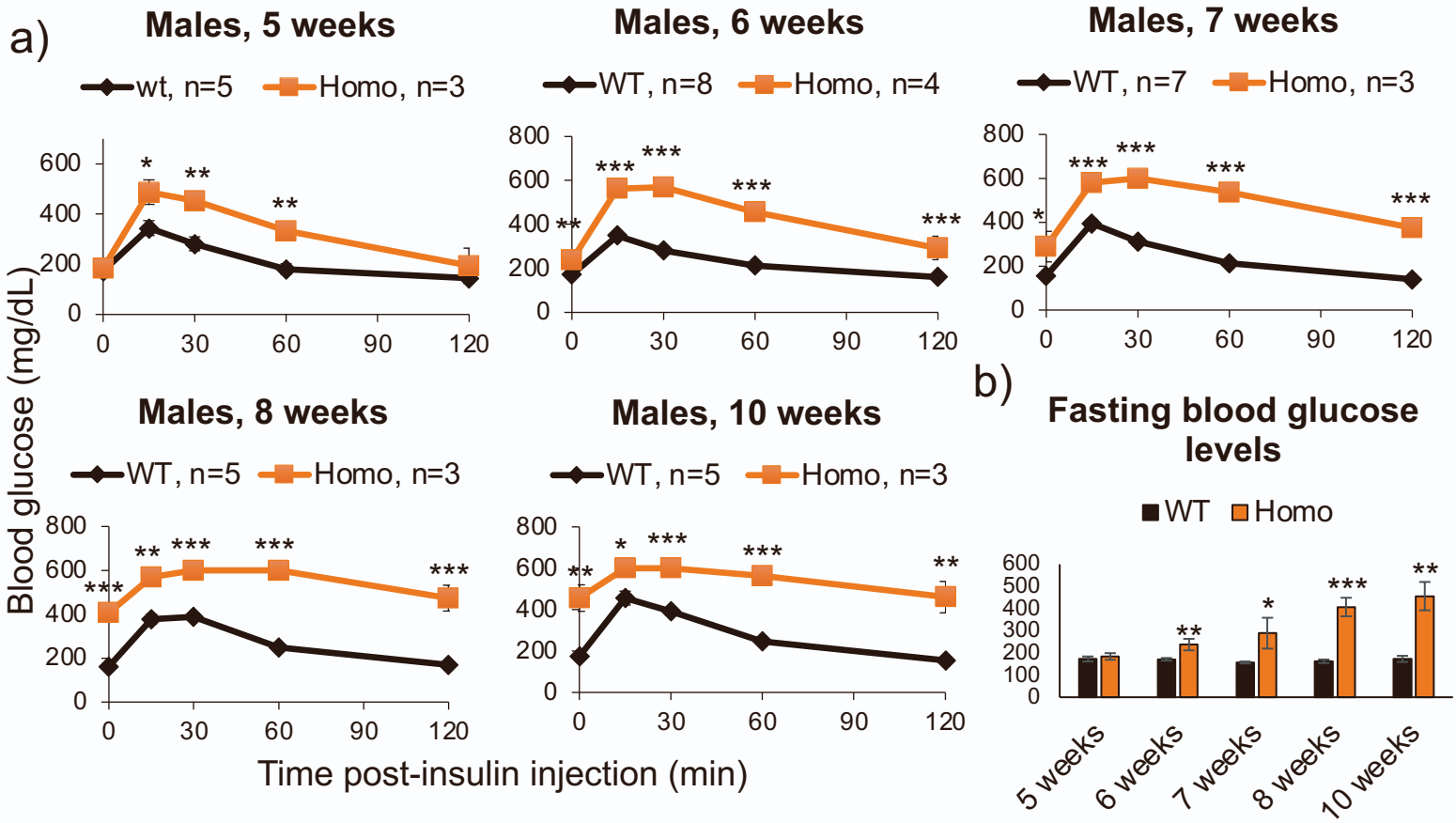

b)

c)

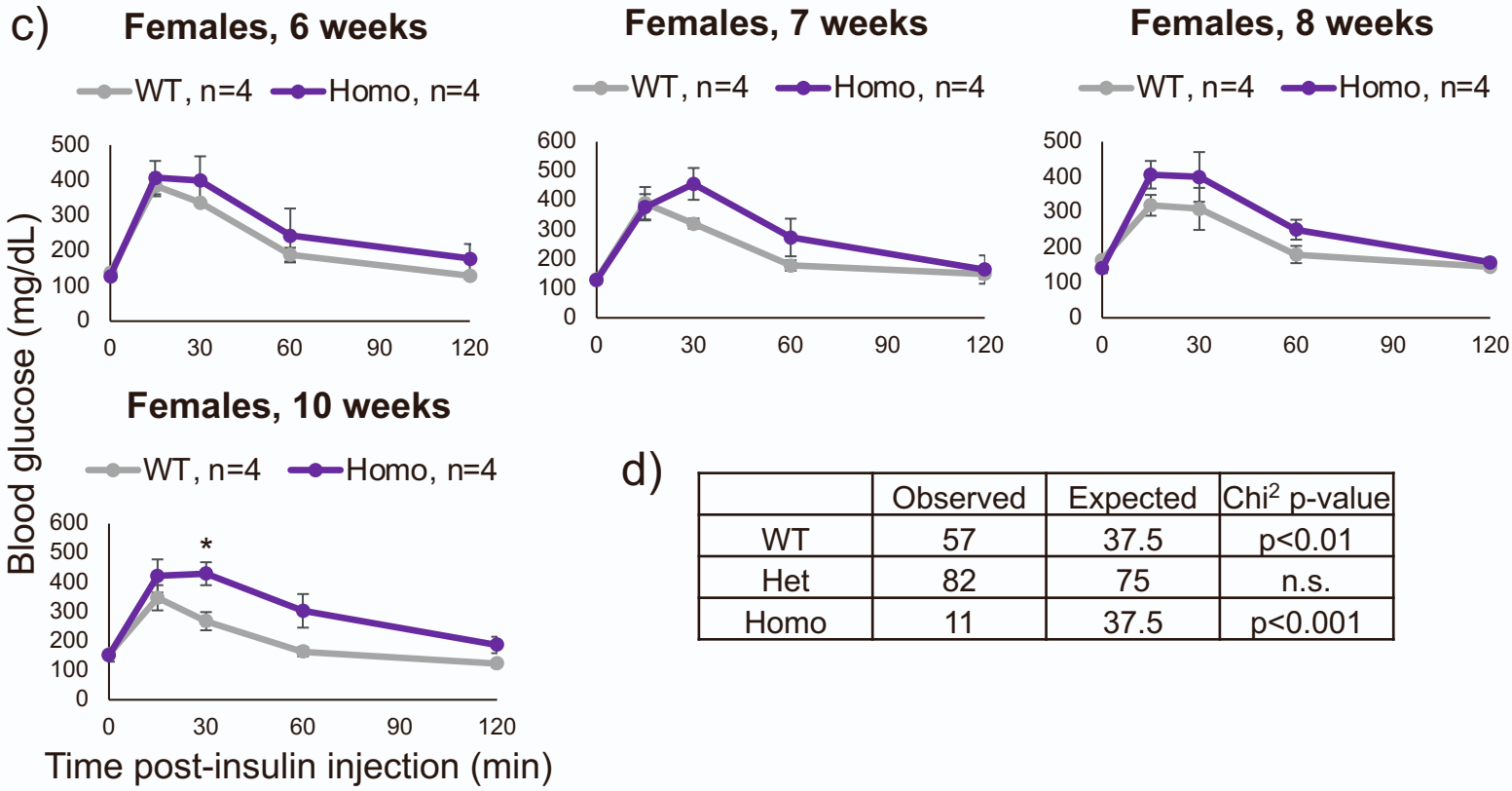

d)

	Observed	Expected	Chi^2 p-value
WT	57	37.5	p<0.01
Het	82	75	n.s.
Homo	11	37.5	p<0.001

Figure S2: Homozygous male *MafA*$^{S64F/S64F}$ mice were hyperglycemic, with glucose tolerance and blood glucose levels worsening with age. Related to Figure 1. a) *MafA*$^{S64F/S64F}$ mice showed progressively worsening glucose tolerance and fasting blood glucose levels between 5 to 10 weeks of age. b) Fasting blood glucose levels in homozygous male mutant mice increased significantly over time. c) Female S64F MafA homozygous mice were only mildly glucose intolerant at 10 weeks of age although their temporal responses to glucose was variable between animals. d) Chi-square analysis revealed that *MafA*$^{S64F/S64F}$ male and female animals were observed with significantly less frequency at weaning than WT animals. In contrast, *MafA*$^{S64F/+}$ numbers were as expected. Two-tail Student *t* test; *p<0.05; **p<0.01; ***p<0.001.

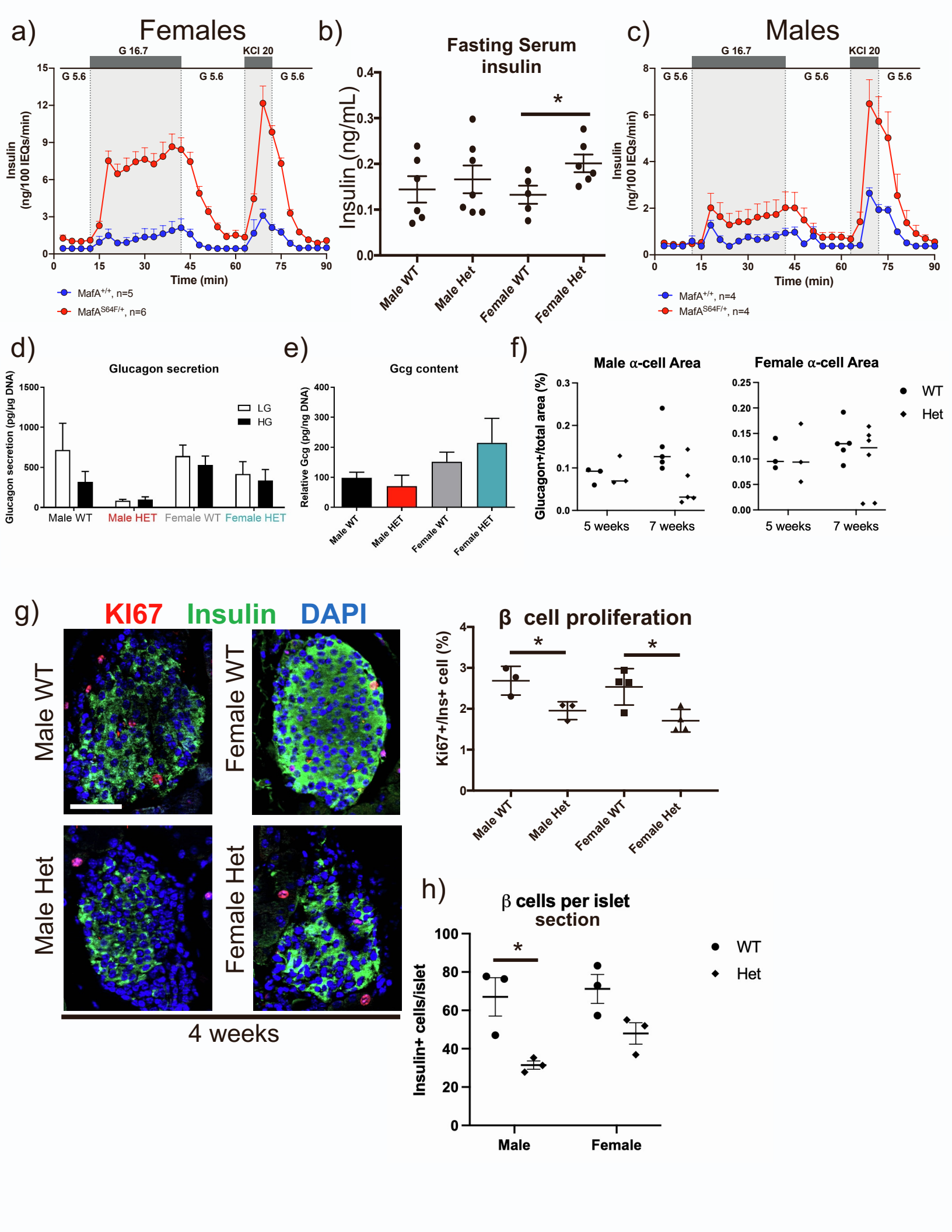
a)
Females
G 16.7
KCl 20
G 5.6
G 5.6
G 5.6
Insulin (ng/100 IEQs/min)
Time (min)
MafA+/+, n=5
MafAS64F/+, n=6
b)
Fasting Serum insulin
Insulin (ng/mL)
*
Male WT
Male Het
Female WT
Female Het
c)
Males
G 16.7
KCl 20
G 5.6
G 5.6
G 5.6
Insulin (ng/100 IEQs/min)
Time (min)
MafA+/+, n=4
MafAS64F/+, n=4
d)
Glucagon secretion
Glucagon secretion (pg/µg DNA)
LG
HG
Male WT
Male HET
Female WT
Female HET
e)
Gcg content
Relative Gcg (pg/ng DNA)
Male WT
Male HET
Female WT
Female HET
f)
Male α-cell Area
Female α-cell Area
Glucagon+/total area (%)
5 weeks
7 weeks
WT
Het
g)
KI67
Insulin
DAPI
Male WT
Female WT
Male Het
Female Het
4 weeks
β cell proliferation
Ki67+/Ins+ cell (%)
*
*
Male WT
Male Het
Female WT
Female Het
h)
β cells per islet section
Insulin+ cells/islet
*
Male
Female
WT
Het

Figure S3: Female and male *MafA*$^{S64F/+}$ islets secreted more insulin in response to high glucose with decreased proliferation and no change in glucagon secretion. Related to Figure 1. a) Islet perifusion demonstrated islets from *MafA*$^{S64F/+}$ female mice secreted higher levels of insulin at low (G 5.6) and high (G 16.7) glucose and in response to KCl. b) Serum insulin levels (ng/mL) were higher in 6-hour fasted female *MafA*$^{S64F/+}$ animals while male *MafA*$^{S64F/+}$ levels were unchanged. c) Islet perifusion results from *MafA*$^{S64F/+}$ male mice at high (G 16.7) glucose and in response to KCl. Islets were isolated from 8-10 week-old animals in both genders. Glucagon secretion (d) and content (e) were unchanged in *MafA*$^{S64F/+}$ islets, which were incubated in 4.6 mM (LG) and 16.7 mM (HG) glucose for 1 hour prior to collection. Secretion and content were normalized to DNA. f) Islet α cell area was not reduced in male or female *MafA*$^{S64F/+}$ mice, though measurements were highly variable between samples. Islet α cell area was calculated by dividing the total glucagon^{+} area by the total pancreas area (eosin staining) multiplied by 100 to obtain percent (%). Two-way ANOVA. g) Representative islets stained for insulin, Ki67 (proliferation marker), and DAPI (nuclei). Islet β cell proliferation was calculated by dividing the number of Ki67^{+} cells by total insulin^{+} β cells. Greater than 1000 β cells were counted per animal. h) β cell number per islet section was significantly reduced in *MafA*$^{S64F/+}$ male mice calculated by dividing the total number of Insulin+ cells by the number of islet sections (n ≥ 20 islets per sample) quantitated. Two-tail Student *t* test; *p<0.05.

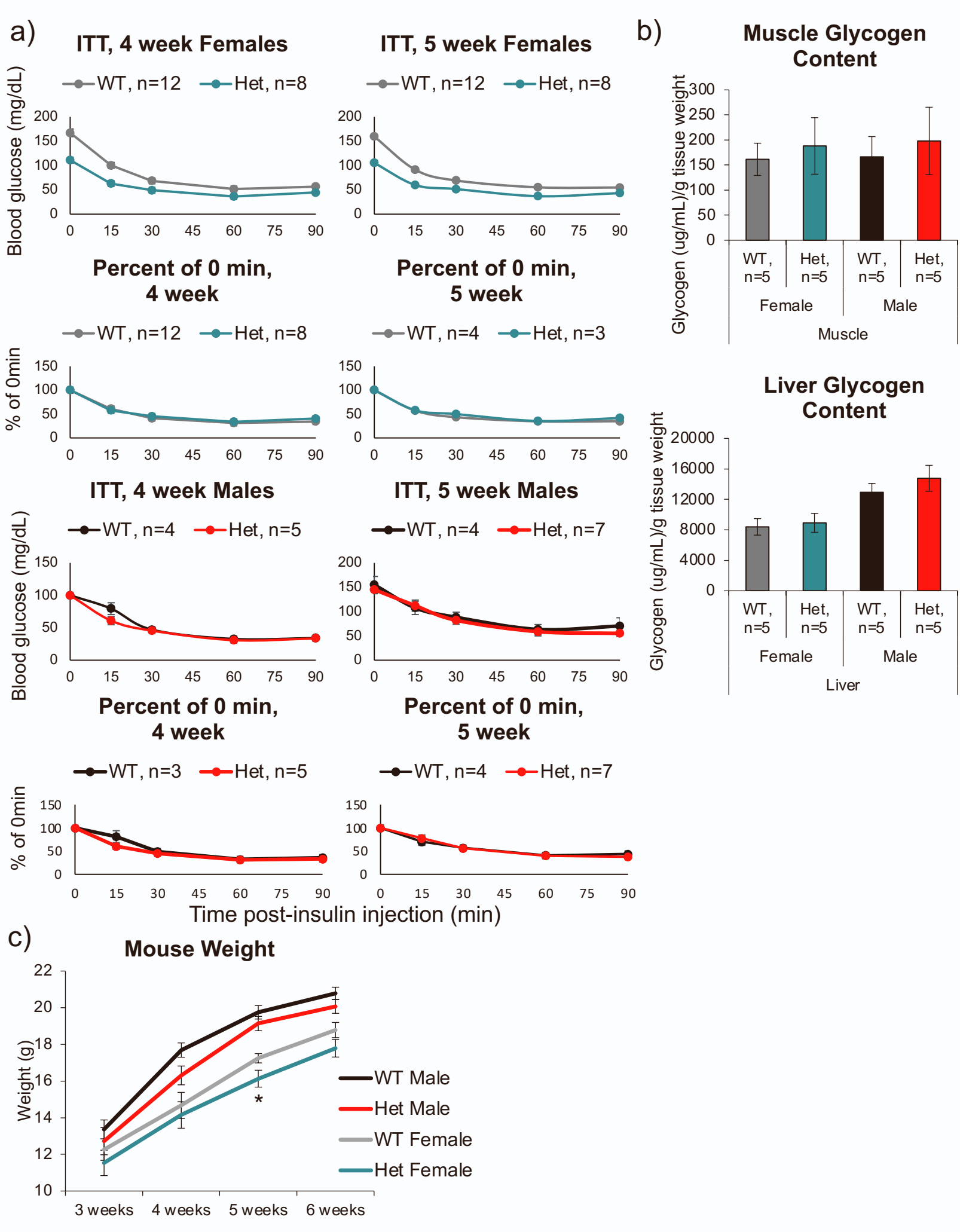
a)
ITT, 4 week Females
ITT, 5 week Females
WT, n=12
Het, n=8
Blood glucose (mg/dL)
Percent of 0 min, 4 week
Percent of 0 min, 5 week
WT, n=4
Het, n=3
% of 0min
ITT, 4 week Males
ITT, 5 week Males
WT, n=4
Het, n=5
Het, n=7
WT, n=3
Time post-insulin injection (min)
b)
Muscle Glycogen Content
Glycogen (ug/mL)/g tissue weight
WT, n=5
Het, n=5
Female
Male
Muscle
Liver Glycogen Content
Liver
c)
Mouse Weight
Weight (g)
3 weeks
4 weeks
5 weeks
6 weeks
WT Male
Het Male
WT Female
Het Female
*

Figure S4: Insulin tolerance and glycogen content are unaltered in *MafA*$^{S64F/+}$ animals. Related to Figure 1. a) Insulin tolerance was unchanged at 4 and 5 weeks in *MafA*$^{S64F/+}$ animals once corrected for initial fasted blood glucose levels (Percent of 0 min). Insulin (0.5U/kg body weight) was injected following a 6-hour fast. b) Glycogen content in muscle (soleus) and liver, normalized to wet tissue weight, was also unaffected in 7-week-old *MafA*$^{S64F/+}$ mice. c) There was no change in average body weight between 3-6 weeks except a small decrease (-1.07-fold) in female *MafA*$^{S64F/+}$ mice at 5 weeks of age. Two-tail Student *t* test; *p<0.05.

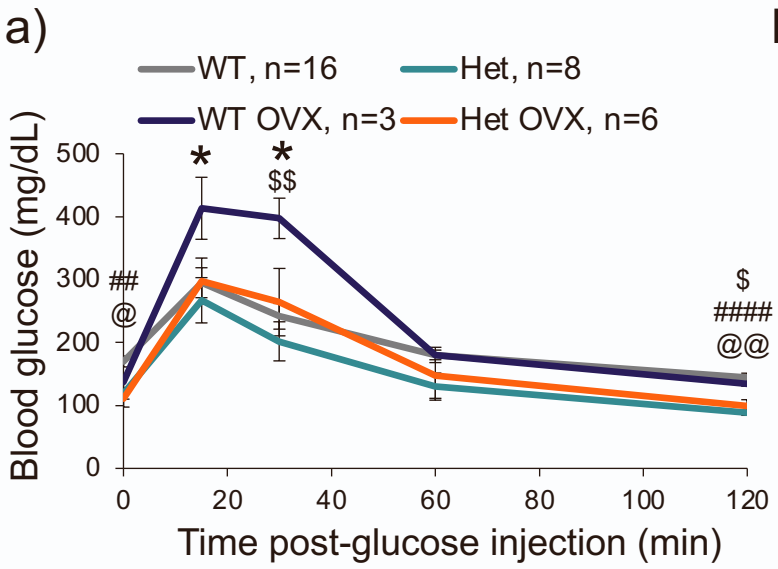
a)
WT, n=16
Het, n=8
WT OVX, n=3
Het OVX, n=6
Blood glucose (mg/dL)
Time post-glucose injection (min)
*
*
$$
##
@
$
####
@@

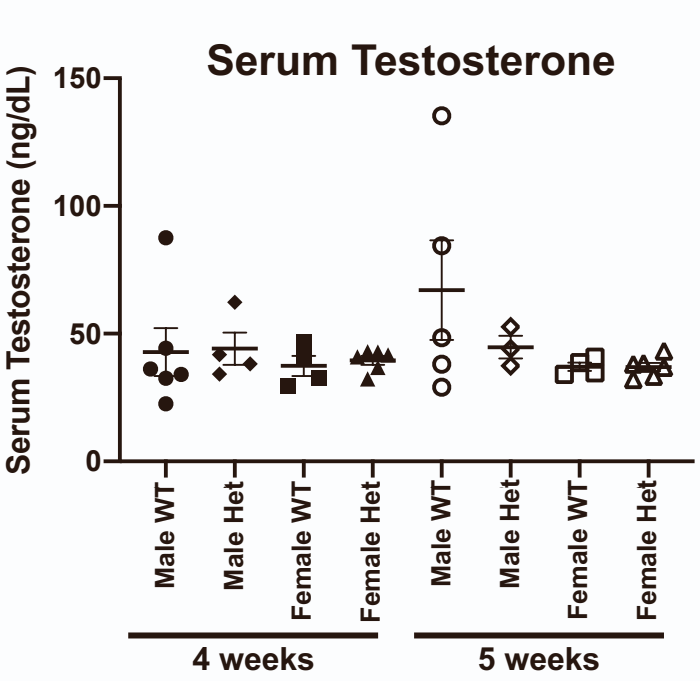
b)
Serum Testosterone
Serum Testosterone (ng/dL)
Male WT
Male Het
Female WT
Female Het
Male WT
Male Het
Female WT
Female Het
4 weeks
5 weeks

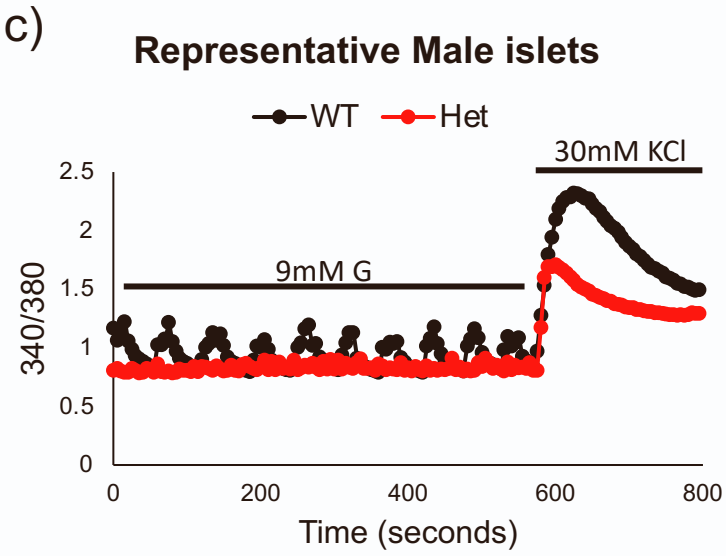
c)
Representative Male islets
WT
Het
30mM KCl
9mM G
340/380
Time (seconds)

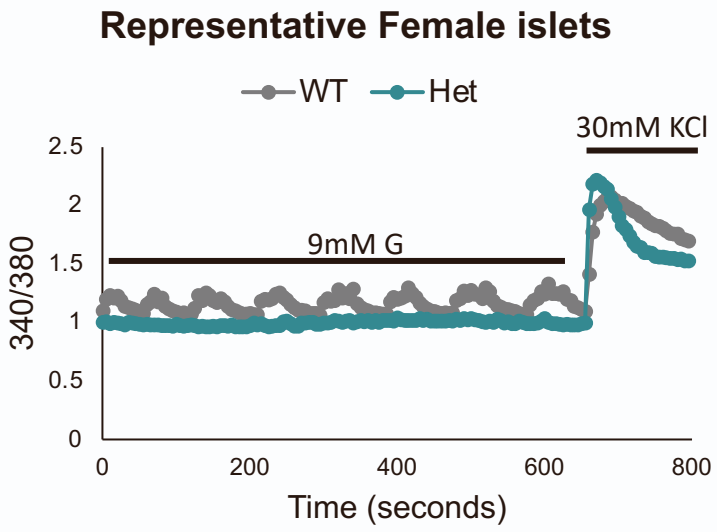
Representative Female islets
WT
Het
30mM KCl
9mM G
340/380
Time (seconds)

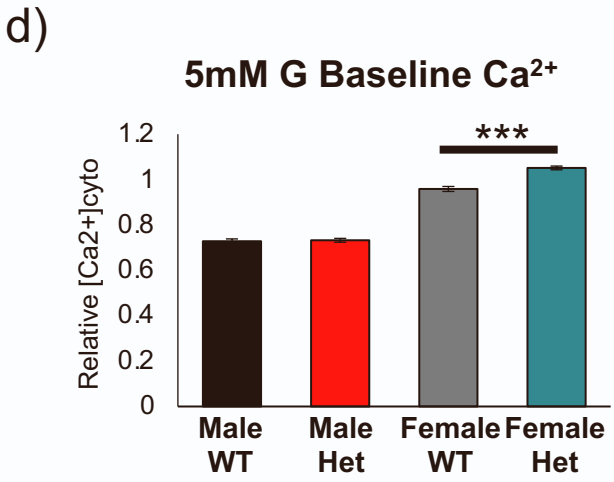
d)
5mM G Baseline Ca2+
***
Relative [Ca2+]cyto
Male WT
Male Het
Female WT
Female Het

Figure S5: Ovariectomy (OVX) did not alter glucose tolerance in female *MafA*$^{S64F/+}$ mice, nor are testosterone levels changed while male *MafA*$^{S64F/+}$ islets had a reduced response to KCl stimulation. Related to Figures 1 and 4. a) Compared to 4-week-old control mice (i.e., non OVX: WT, grey line; Het, teal line), the GTT at 1-week post ovariectomy showed glucose intolerance in WT female mice (WT OVX, purple line) and no change in *MafA*$^{S64F/+}$ mice (Het OVX, orange line). One-way ANOVA; WT vs. WT OVX: *p<0.05; Het vs. WT OVX: $^{\$}$p<0.05; $^{\$\$}$p<0.01; WT vs. Het: $^{\#\#}$p<0.01; $^{\#\#\#\#}$p<0.0001; WT vs. Het OVX: $^{@}$p<0.05; $^{@@}$p<0.01. b) Serum testosterone levels were unchanged in male or female *MafA*$^{S64F/+}$ mice. Male and female testosterone levels are similar at 4 and 5 weeks of age. Two-way ANOVA. c) Representative Ca^{2+} traces quantitated in Figure 4c in response to both high glucose (9 mM) and KCl (30 mM). d) Female *MafA*$^{S64F/+}$ islets have increased baseline Ca^{+2} at 5mM compared with WT islets (right) while male *MafA*$^{S64F/+}$ islets do not (left).

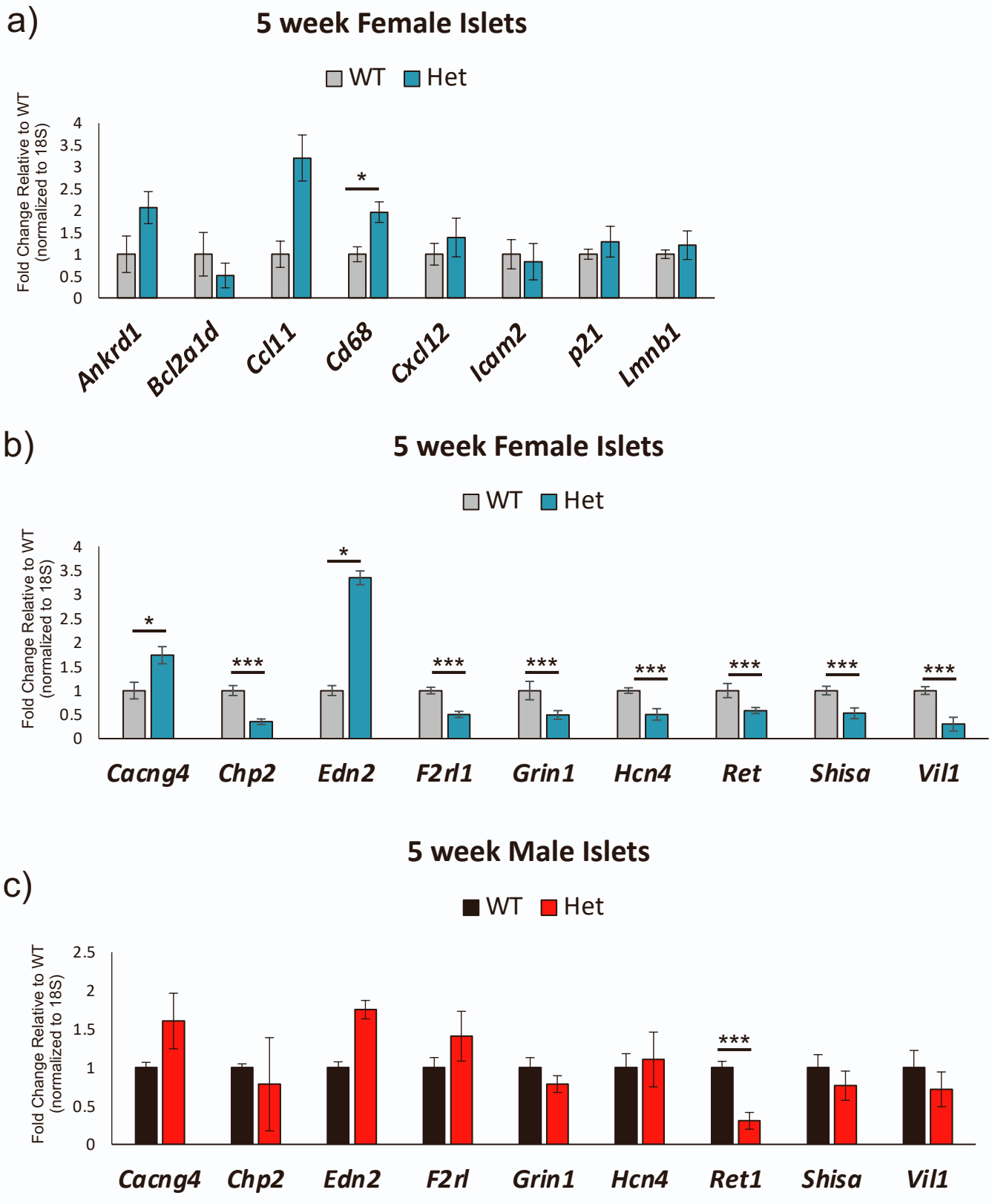

Figure S6: qPCR confirmation of changes in islet gene expression identified by RNA-seq. Related to Figure 5. a) Senescence markers were primarily unchanged in female *MafA*$^{S64F/+}$ islets. b-c) Genes altered specifically in female *MafA*$^{S64F/+}$ islets (b) identified by RNA-seq were mostly unchanged in male *MafA*$^{S64F/+}$ islets (c). Two-tail Student *t* test; *p<0.05; ***p<0.001.

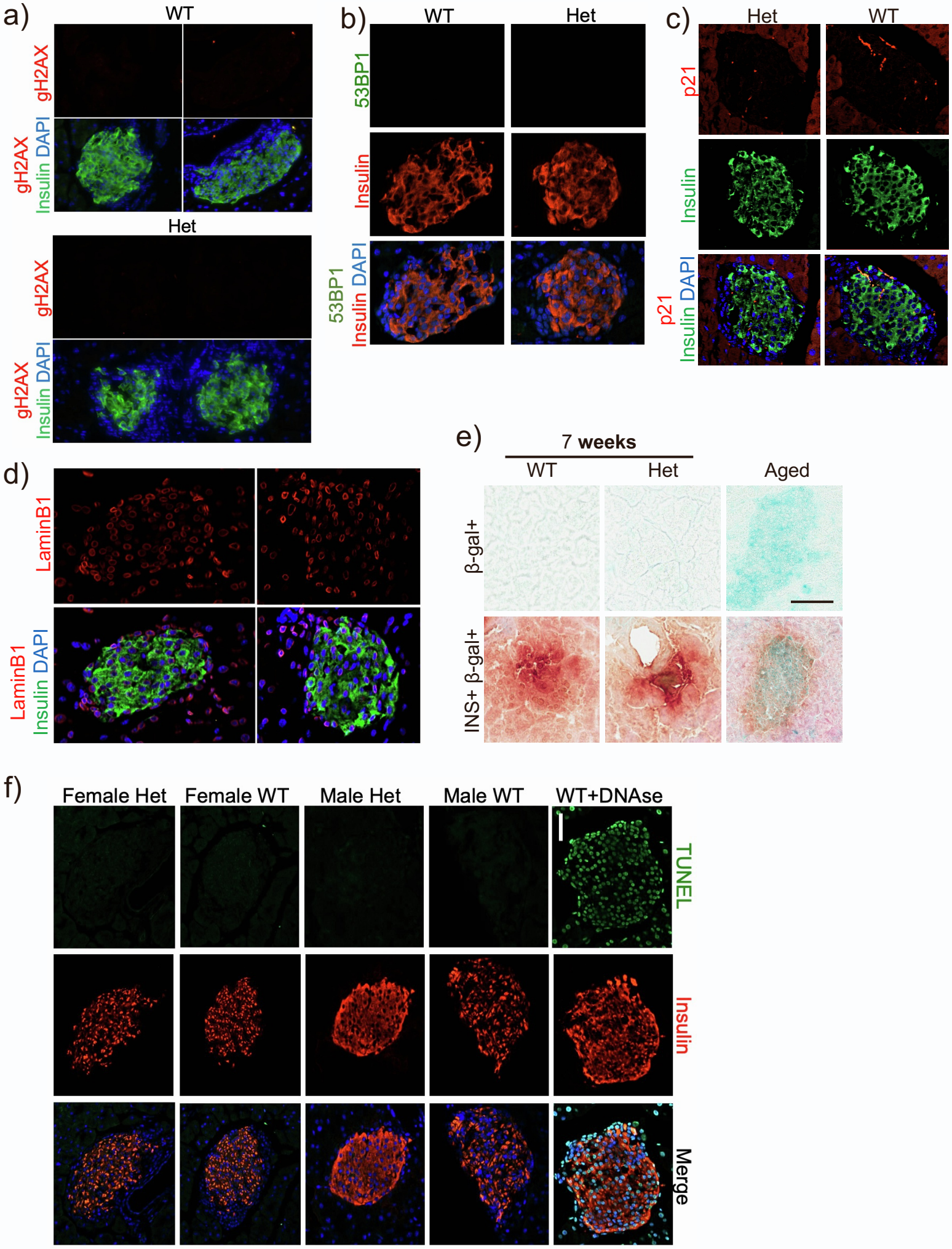
a)
WT
gH2AX
gH2AX
Insulin DAPI
Het
gH2AX
gH2AX
Insulin DAPI
b)
WT
Het
53BP1
Insulin
53BP1
Insulin DAPI
c)
Het
WT
p21
Insulin
p21
Insulin DAPI
d)
LaminB1
LaminB1
Insulin DAPI
e)
7 weeks
WT
Het
Aged
β-gal+
INS+ β-gal+
f)
Female Het
Female WT
Male Het
Male WT
WT+DNAse
TUNEL
Insulin
Merge

Figure S7: DNA damage and cell cycle inhibition markers were not detected in 5-week-old female *MafA*$^{S64F/+}$ islets, nor were significant levels of apoptosis found in *MafA*$^{S64F/+}$ islet cells. Related to Figure 6. a-e) Changes in immunostaining for γH2AX (DNA double strand break; a), 53BP1 (DNA double strand break; b), p21 (cell cycle inhibitor; c), LaminB1 protein (nuclear integrity marker; d) and endogenous staining for SA-β-gal (senescence marker; e) were not altered in female *MafA*$^{S64F/+}$ islets. f) TUNEL^{+} nuclei were barely detected in *MafA*$^{S64F/+}$ islets at 6 weeks of age but easily visible in DNase treated controls (top panels).

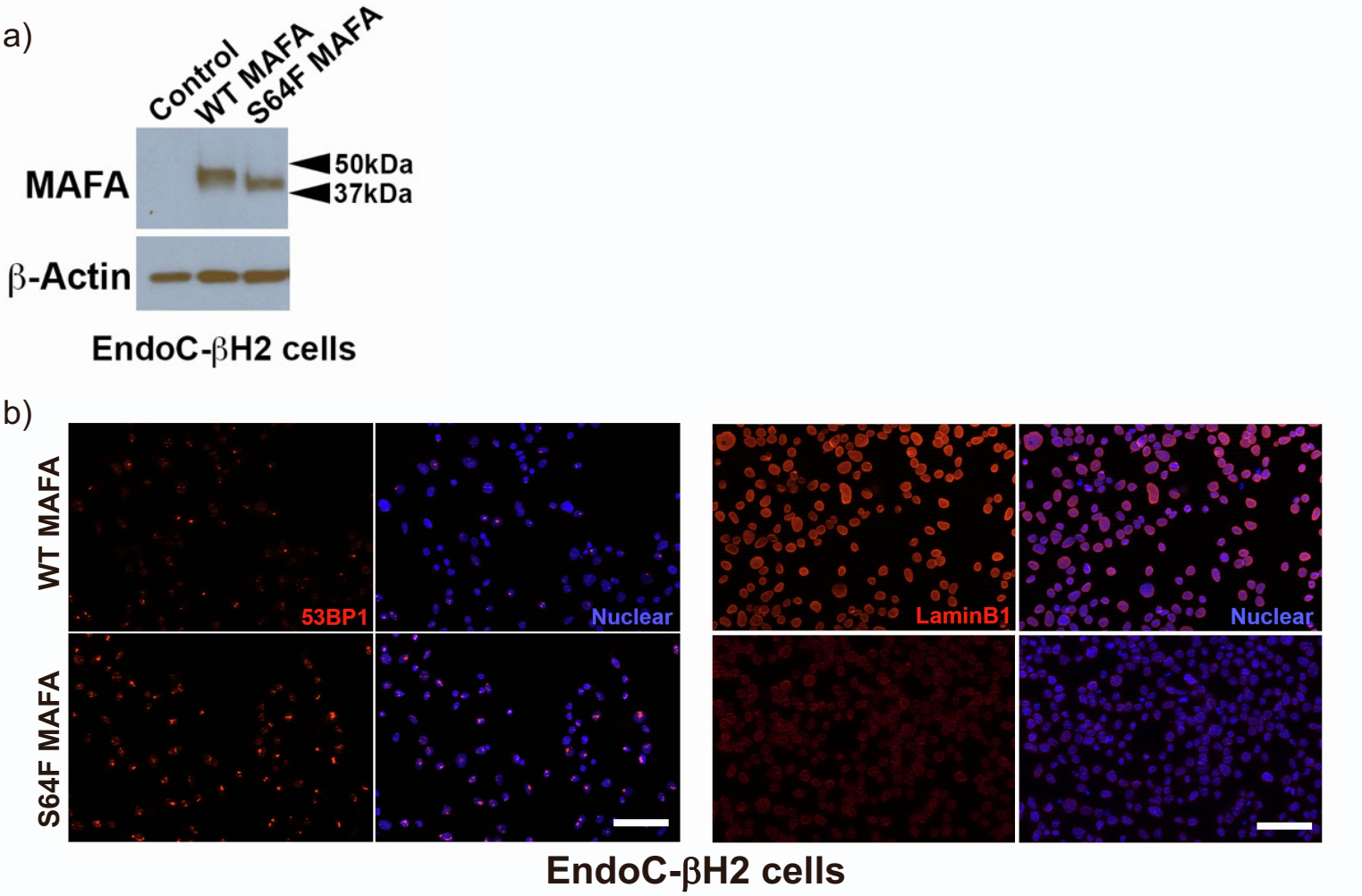

Figure S8: MAFA^{S64F} expressing human cells have changes in DNA damage, senescence, and Ca^{2+} channel gene expression. Related to Figure 7. a) Western blotting for EndoC-βH2 cells transduced to express WT MAFA or MAFA^{S64F} shows faster migration in the MAFA^{S64F} lane consistent with under-phosphorylated MAFA. Higher MAFA^{S64F} protein level is likely due to increased MAFA protein stability seen in (Iacovazzo et al., 2018). b) 53BP1 staining (left) intensity was higher and LaminB1 staining (right) intensity was lower in MAFA^{S64F} expressing EndoC-βH2 cells compared with MAFA^{WT}. c) qRT-PCR for Ca^{2+} channel genes (left) showed some alterations in MAFA^{S64F} expressing EndoC-βH2 cells while no changes in insulin secretion machinery genes were detected, consistent with findings in *MafA*$^{S64F/+}$ mouse islets.

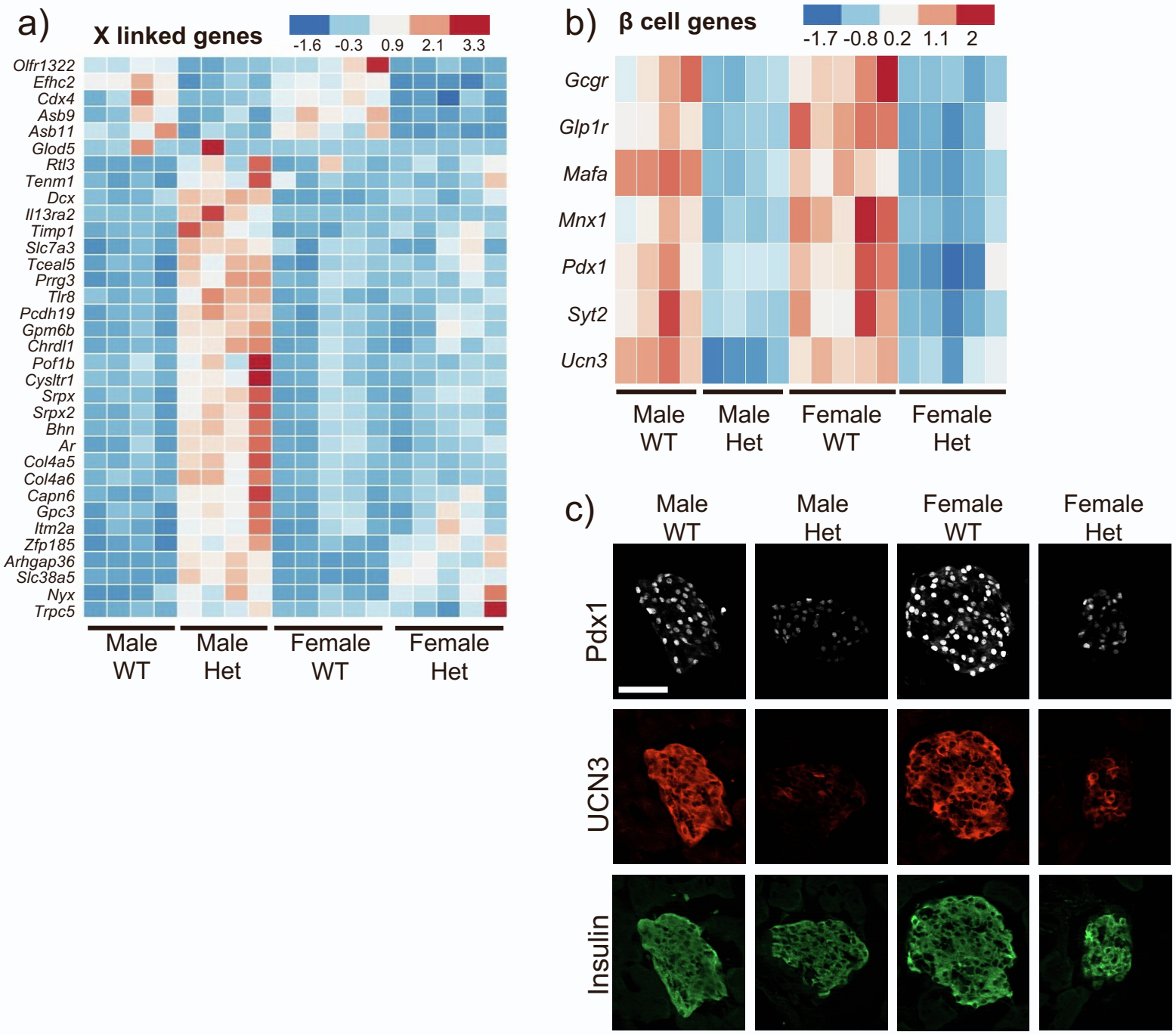

Figure S9: Many X chromosome linked genes were altered in male *MafA*$^{S64F/+}$ islets and production of some β cell identity gene products are downregulated in both male and female *MafA*$^{S64F/+}$ islets. Related to Figure 3. a) Heat map developed from the 5-week-old islet RNA-Seq data. FDR<0.05. b) Heat map showing β identity genes decreased in both male and female Het islets. FDR<0.05. c) Immunostaining illustrating decreased Pdx1 and Ucn3 protein levels in 7-week-old Het islets.

Table S1: Primer information

Mouse primers	Forward	Reverse
MafA	CCTGTAGAGGAAGCCGAGGAA	CCTCCCCCAGTCGAGTATAGC
Ins1	CACTTCCT ACCCCTGCTGG	ACCACAAAGATGCTGTTTGACA
pre-Ins2	GGGGAGCGTGGCTTCTTCTA	GGGGACAGAATTCAGTGGCA
Ins2	CCACCCAGGCTTTTGTCAAA	CCCAGCTCCAGTTGTTCCAC
Pdx1	CGGCTGAGCAAGCTAAGGTT	TGGAAGAAGCGCTCTCTTTGA
Ucn3	AGCACCCGGTACAGATACCAA	GGCCTTGTCGATGTTGAAGAG
Ankrd1	AAACGGACGGCACTCCACCG	CGCTGTGCTGAGAAGCTTGTCTCT
Bcl2a1d	GTATATCCACTCCCTGGCTGAG	TAGTCACAATCCTTCCCCAGTT
Ccl11	TCCACAGCGCTTCTATTCCTG	GGAGCCTGGGTGAGCCA
Cd68	ACTTCGGGCCATGTTTCTCT	GCTGGTAGGTTGATTGTCGT
Cxcl12	CAGTGACGGTAAACCAGTCAGC	TGGCGATGTGGCTCTCG
Icam1	CAATTTCTCATGCCGCACAG	AGCTGGAAGATCGAAAGTCCG
p21	GCCTTAGCCCTCACTCT TG	AGCTGGCCTTAGAGGTGACA
Cacng4	TCCGGAAGACGCGGACTAC	ATGATGTTGTGGCGTGTCTTG
Chp2	CGCCTAGACCTCCAGCAGATC	GCCTGCGAAATACAGTCTCTGAC
Edn2	CTGGCAAGATGTGGACTGCTGA	GCCTTTCTTGTCACCTCTGGCT
F2rl1	CGGACCGAGAACCTTGCACCG	GTGAGGATGGACGCAGAGAACT
Grin1	CCTTTCAGAGCACACTGTGGCT	CCAGGAAAACCACATGGCAGAG
Hcn4	CGTGCTCACTAAGGGCAACAAAG	GCACCTCATTGAAGTTGTCCACG
Ret	TTCCAGCATCAACTGCACTG	GTCAGTGGCTACCACCGTGT
Shisa2	TGCGACAACGACCGCCAGCAG	TGAAGGCAACGAACACTGAGCC
Vil1	TTCTACGGTGGTGACTGCTACC	TGGTCCAACAGGACGGCTTGAT
18S rRNA	GTAACCCGTTGAACCCCATT	CCATCCAATCGGTAGTAGCG
Lmnb1	CAGGAATTGGAGGACATGCT	GAAGGGCTTGGAGAGAGCTT
β-Actin	AGGTCATCACTATTGGCAACGA	CACTTCATGATGGAATTGAATGTAGTT

Human primers	Forward	Reverse
MAFA	GAGAGCGAGAAGTGCCAACT	TTCTCCTTGTACAGGTCCCG
MAFB	CATAGAGAACGTGGCAGCAA	ATGCCCGGAACTTTTTCTTT
INS	AGAGGCCATCAAGCAGATCACTGT	ACAGGTGTTGGTTCACAAAGGCTG
ANKRD1	AGACTCCTTCAGCCAACATGATG	CTCTCCATCTCTGAAATCCTCAGG
BCL2A1	GGATAAGGCAAAACGGAGGCTG	CAGTATTGCTTCAGGAGAGATAGC
CCL11	GCTACAGGAGAATCACCAGTGG	GGAATCCTGCACCCACTTCTTC
CD68	CGAGCATCATTCTTTCACCAGCT	ATGAGAGGCAGCAAGATGGACC
CXCL12	CTCAACACTCCAAACTGTGCCC	CTCCAGGTACTCCTGAATCCAC
ICAM1	AGCGGCTGACGTGTGCAGTAAT	TCTGAGACCTCTGGCTTCGTCA
P21	CCTGTCACTGTCTTGTACCCT	GCGTTTGGAGTGGTAGAAATCT
BCL2	ATCGCCCTGTGGATGACTGAGT	GCCAGGAGAAATCAAACAGAGGC
CXCL2	GGCAGAAAGCTTGTCTCAACCC	CTCCTTCAGGAACAGCCACCAA
ICAM3	AGATCGTCTGCAACGTGACCCT	TCGCTGAGGTTCACAATGGGTC
IGFBP2	CGAGGGCACTTGTGAGAAGCG	TGTTCATGGTGCTGTCCACGTG
IGFBP4	GAGCTGGGTGACACTGCTTG	CCCACGAGGACCTCTACATCA
IGF1R	CTCCTGTTTCTCTCCGCCG	ATAGTCGTTGCGGATGTCGAT
LMNB1	TGGAGTGG TTGTTGAGGAAG	GAGAAGGCTCTGCACTGTATAC
CACNA1A	CTGGTAGCCTTTGCCTTCACTG	ACACAGCCTTGAGCTTTGGCAG
CACNA1C	GCAGGAGTACAAGAACTGTGAGC	CGAAGTAGGTGGAGTTGACCAC
CACNA1E	AGCGTGAGACAGGCAAAGCCAT	GGATGCACATCTCAAAGTAGCGC
CACNA1G	TTCACCGCAGTCTTTCTGGCTG	TGACGGAGATGAGCACCAACAG
EXOC3	GAGCCATTGCTTTCTCCACACG	TGGCTCTGTCTCTTTGACCCAG
EXOC5	CTTCAGTAATCCAGAAACAGTCCT	TGCTCTGCATCGGACTTCCTAC
SNAP25	CGTCGTATGCTGCAACTGGTTG	GGTTCATGCCTTCTTCGACACG
VAMP2	CTCCAAACCTCACCAGTAACAGG	AGCTCCGACAGCTTCTGGTCTC
STX1A	GGAACACGCGGTAGACTATGT	CTGGAGTGGAGTGGCAGTTT
KCNJ11	TGTGTCACCAGCATCCACTCCT	GTTCTGCACGATGAGGATCAGG
GAPDH	CTCACCGGATGCACCAATGTT	CGCGTTGCTCACAATGTTCAT